

# A mineralogical investigation into the pre-concentration of the Nechalacho deposit by gravity separation

Marion, Christopher; Grammatikopoulos, Tassos; Rudinsky, S.; Langlois, Ray; Williams, Hillary; Chu, P.; Awais, Muhammad; Gauvin, R.; Rowson, Neil; Waters, K. E.

DOI:

[10.1016/j.mineng.2018.02.008](https://doi.org/10.1016/j.mineng.2018.02.008)

License:

Creative Commons: Attribution-NonCommercial-NoDerivs (CC BY-NC-ND)

*Document Version*

Peer reviewed version

*Citation for published version (Harvard):*

Marion, C, Grammatikopoulos, T, Rudinsky, S, Langlois, R, Williams, H, Chu, P, Awais, M, Gauvin, R, Rowson, N & Waters, KE 2018, 'A mineralogical investigation into the pre-concentration of the Nechalacho deposit by gravity separation', *Minerals Engineering*, vol. 121, pp. 1-13. <https://doi.org/10.1016/j.mineng.2018.02.008>

[Link to publication on Research at Birmingham portal](#)

## **Publisher Rights Statement:**

Published in *Minerals Engineering* on 06/03/2018

DOI: 10.1016/j.mineng.2018.02.008

## **General rights**

Unless a licence is specified above, all rights (including copyright and moral rights) in this document are retained by the authors and/or the copyright holders. The express permission of the copyright holder must be obtained for any use of this material other than for purposes permitted by law.

- Users may freely distribute the URL that is used to identify this publication.
- Users may download and/or print one copy of the publication from the University of Birmingham research portal for the purpose of private study or non-commercial research.
- User may use extracts from the document in line with the concept of 'fair dealing' under the Copyright, Designs and Patents Act 1988 (?)
- Users may not further distribute the material nor use it for the purposes of commercial gain.

Where a licence is displayed above, please note the terms and conditions of the licence govern your use of this document.

When citing, please reference the published version.

## **Take down policy**

While the University of Birmingham exercises care and attention in making items available there are rare occasions when an item has been uploaded in error or has been deemed to be commercially or otherwise sensitive.

If you believe that this is the case for this document, please contact [UBIRA@lists.bham.ac.uk](mailto:UBIRA@lists.bham.ac.uk) providing details and we will remove access to the work immediately and investigate.

# A Mineralogical Investigation into the Pre-Concentration of the Nechalacho Deposit by Gravity Separation

C. Marion<sup>1</sup>, T. Grammatikopoulos<sup>2</sup>, S. Rudinsky<sup>1</sup>, R. Langlois<sup>1</sup>, H. Williams<sup>1</sup>, P. Chu<sup>1</sup>,  
M. Awais<sup>3</sup>, R. Gauvin<sup>1</sup>, N.A. Rowson<sup>3</sup> and K.E. Waters<sup>1\*</sup>

<sup>1</sup>*Department of Mining and Materials Engineering, McGill University  
3610 University Street  
Montreal, Canada H3A 0C5  
(\*Corresponding author: kristian.waters@mcgill.ca)*

<sup>2</sup>*SGS Canada Inc.  
185 Concession Street  
Lakefield, Canada K0L 2H0*

<sup>3</sup>*School of Chemical Engineering, University of Birmingham  
Edgbaston  
Birmingham, UK B15 2TT*

## Abstract

The Nechalacho rare earth element (REE) deposit is located in the Northwest Territories, Canada. Of the various REE-bearing minerals in the deposit, zircon is significant due to its elevated heavy rare earth element (HREE) content. Most studies performed on this ore to date have focused on fully liberating REE-bearing minerals through fine grinding prior to a separation stage. However, previous lab scale work has shown that zircon can be concentrated in relatively coarse sizes, suggesting the potential to pre-concentrate the ore by gravity separation without complete liberation. The current work investigates the pre-concentration of the Nechalacho deposit using a spiral concentrator and a Knelson Concentrator on a relatively coarse ( $d_{80} = 97 \mu\text{m}$ ) feed. The feed sample and the resultant fractions, produced by each separation technique, were analyzed with ICP-MS to determine the zirconium and REE content. The samples were also analyzed with QEMSCAN, to identify the effect of particle size, mineral liberation and association characteristics, and mineral particle SG distributions on each gravity separation technique. The results suggest that the value minerals can be effectively concentrated by gravity separation even when they are poorly liberated. It is important to note that the process examined here is not representative of the currently selected process design or recovery for the Nechalacho deposit. Any application of this process to this deposit would require optimization to ensure appropriate grade and recovery targets are met.

## Keywords

Rare Earth Elements; Zircon; Gravity Concentration; QEMSCAN; Pre-Concentration

# 1. Introduction

## 1.1 Rare Earth Elements

The rare earth elements (REE), which encompass the 15 elements of the lanthanide series of the periodic table of elements, plus yttrium (Y), are strategic metals which are indispensable to the development of modern defense systems, electronic applications and green technologies. The growing economic and strategic importance of these sectors, coupled with uncertainty in the global supply of REE from China (highlighted by the implementation of export quotas in 2010), have led to concerns about the future supply of many of these metals (Paulick and Machacek, 2017; Weng *et al.*, 2015). The severity of the supply concerns varies strongly among the various REE. Although their overall demand is much lower, heavy rare earth elements (HREE) [europium (Eu) through lutetium (Lu) and Y] are considered to have a greater supply risk than light rare earth elements (LREE) [lanthanum (La) through samarium (Sm)] because they are much less abundant in the earth's crust and are highly important in many high-technology and clean energy applications (Golev *et al.*, 2014; Paulick and Machacek, 2017). The production of neodymium (Nd), Eu, terbium (Tb), dysprosium (Dy) and Y (all of which are classified as HREE with the exception of Nd) has been declared to be most critical (Seredin, 2010; U.S. Department of Energy, 2011). Due to these supply concerns and the increasing demand of REE, many new rare earth mineral (REM) deposits are being investigated. One such deposit is the Nechalacho (owned by Avalon Advanced Materials Inc.) in the Northwest Territories (Canada). It is one of the largest REE projects outside of China, with inferred resources of 183.4 million tonnes at a grade of 1.27 % total rare earth oxide (REO) and 0.17 % heavy rare earth oxide (HREO) (Ciuculescu *et al.*, 2013).

## 1.2 Pre-Concentration and Gangue Rejection

Pre-concentration is a processing step aimed at rejecting waste early in the concentration process. Earlier rejection of gangue can have significant benefits, including increased feed grades to downstream processes, and lower ore throughputs and operating costs. Ores amenable to pre-concentration at coarser particle sizes would also benefit from lower energy requirements in the comminution stage. The method of separation used to reject gangue material during pre-concentration is dependent on the physical properties of the ore and often rely on differences in specific gravity (SG), color, particle size, radioactivity, conductivity, or magnetic susceptibility between valuable material and gangue. Gravity separation is a common pre-concentration step for many REM deposits (especially heavy mineral sands deposits), focussed on rejecting low SG gangue material (Gupta and Krishnamurthy, 2005; Jordens *et al.*, 2013; Zhang and Edwards, 2012). A brief discussion on gravity separation is presented here, but a more detailed review of all beneficiation

techniques pertaining to REM deposits can be found in Jordens *et al.* (2013) and Zhang and Edwards (2012).

### 1.3 Gravity Concentration

Gravity concentration is the separation of minerals based upon differences in SG. It offers multiple advantages over other separation techniques, such as flotation. Gravity separation techniques generally have low capital and operational costs (no reagent costs), comparatively little environmental impact and are relatively simple processes (Wills and Finch, 2016a). Along with SG differences, particle size and shape often play a role in separation. The various gravity concentration techniques can be classified as either conventional or enhanced gravity separators. Enhanced gravity separators, or centrifugal gravity separators, such as the Knelson Concentrator, induce an artificially high gravitational force on the particles, amplifying differences in SG. This allows enhanced gravity techniques to be much more effective at recovering fine particles and processing relatively low SG minerals than conventional gravity separators (Wills and Finch, 2016a). Although conventional gravity separators, such as spiral concentrators, are limited to processing relatively coarse (>53 µm) material, they offer advantages in increased throughputs, greater simplicity (centrifugal devices are mechanical, whereas conventional techniques are not), and they are better suited for higher grade (>1 % heavy material) deposits due to the semi-continuous nature of most centrifugal bowl separators (Richards *et al.*, 2000; Wills and Finch, 2016a).

### 1.4 Pre-Concentration of REM in the Nechalacho Deposit

The main REE-bearing minerals in the Nechalacho deposit are zircon, allanite, bastnäsite, synchysite, monazite, columbite (Fe) and fergusonite. The major gangue minerals are quartz, feldspars and iron (Fe) oxides. Zircon is of significant importance, due to its high HREE content compared to other REMs in the deposit (Ciuculescu *et al.*, 2013; Grammatikopoulos *et al.*, 2011). Most of the work performed on this ore to date has focused on fully liberating REE-bearing minerals through fine grinding prior to a separation stage (Jordens *et al.*, 2016a; Jordens *et al.*, 2016b; Jordens *et al.*, 2016c; Jordens *et al.*, 2014; Xia *et al.*, 2015a; Xia *et al.*, 2015b). Recently, Jordens *et al.* (2016b) and Jordens *et al.* (2016c) studied the use of gravity and magnetic separation to produce a high-grade REE concentrate of a Nechalacho feed ground to 80 % passing 40 µm. They demonstrated that centrifugal gravity concentration, particularly using a Knelson concentrator, was effective at pre-concentrating REM in this deposit. One major finding from this work was that, following grinding, particles coarser than 20 µm were enriched in zircon. They also noted that grain size differences in the deposit may present opportunities for selective comminution and subsequent upgrading of the concentrated coarse material by gravity separation.

## 1.5 Paper Objectives

This work investigates the use of gravity separation to pre-concentrate the Nechalacho deposit, building upon the findings of Jordens *et al.* (2016b) and Jordens *et al.* (2016c). The aim of this paper is to study the effects of particle size, mineral liberation and association characteristics, and mineral particle SG distributions on the separation performance of a Knelson Concentrator and a spiral concentrator of a relatively coarse Nechalacho feed. Producing a high-grade zircon pre-concentrate, at coarser particle sizes, would present opportunities to minimise grinding costs prior to a primary separation stage. It is important to note that the process examined here is not representative of the currently selected process design or recovery for the Nechalacho deposit. Any application of this process to the deposit would require optimization to ensure appropriate grade and recovery targets are met.

## 2. Materials and Methods

### 2.1 Materials

The ore used in this work was obtained from the Nechalacho deposit (Avalon Advanced Materials Inc., Canada). A 50 kg sample of ore, with an initial top size of 3.36 mm, was riffled to produce 1 kg representative samples. Samples were then ground wet at 50 %<sub>w/w</sub> solids using a laboratory ball mill for 40 min to produce a particle size distribution of 94 % passing 106 µm (80 % passing 70 µm; 60 % passing 38 µm). The mill products were subsequently combined and sieved wet at 38 and 53 µm to completely remove the - 38 µm material and the majority of - 53 µm particles, and at 800 µm to remove very coarse material from the feed. This resulted in a relatively coarse gravity feed with a narrow size distribution ( $d_{80} = 97 \mu\text{m}$ ,  $d_{50} = 72 \mu\text{m}$ ). The particle size distribution of the feed sample is shown in Appendix A (Figure A1). As a significant amount of valuable material would be lost in the removed fine particle fraction, a secondary stream would be required for processing this size class. However, through a strategic grinding and classification circuit the recovery of material in the desired size fraction could be potentially improved. The sample was then representatively split into two 5 kg samples, which were fed to the spiral and Knelson Concentrator and one 45 g sample for dense medium separation (DMS).

### 2.2 Dense Medium Separation

DMS is a process by which minerals are separated based on differences in SG. The process utilizes a liquid or an aqueous suspension of fine particles with a predetermined density for which particles less dense than the liquid will float while those heavier will sink. This work used a heavy liquid solution [lithium metatungstate (LMT), purchased from LMT Liquid, LLC (USA)] as the dense medium.

1 An important consideration for DMS is particle size. When using centrifugal separators, DMS is  
2 effective at processing material down to 0.5 mm, which is significantly coarser than the gravity feed  
3 produced in this work. However, in lab-scale DMS, particle size is not a factor and sharp separations  
4 remain possible at fine particle sizes (Browning, 1961). In this case, it is likely not economical as a  
5 large-scale separation process, but, DMS is an effective method to determine the feasibility of  
6 gravity separation on ores. For an overview of the DMS process, interested readers are referred to  
7 Napier-Munn *et al.* (2014) and Wills and Finch (2016b).  
8  
9

10 To perform DMS on the gravity feed, three 15 g representative samples were added to 50 mL  
11 centrifuge tubes along with 30 mL of heavy liquid solution with an SG of 2.95. The suspensions were  
12 then mixed by hand shaking and centrifuged for 30 min at 4400 rpm using a IEC Centra CL2  
13 centrifuge (Thermo Electron Corporation, USA). After centrifuging, the float fraction on the liquid  
14 surface was poured off along with the heavy liquid solution leaving the sink fraction behind. The  
15 float and sink fractions were then filtered, thoroughly washed, dried and weighed. The float fraction  
16 was then subsequently reprocessed following the same steps, but, using a heavy liquid solution with  
17 SG 2.75. Float and sink fractions were then analyzed by inductively coupled plasma mass  
18 spectrometry (ICP-MS) and scanning electron microscopy (SEM).  
19  
20  
21  
22  
23  
24  
25  
26  
27  
28

## 29 **2.3 Spiral Concentration**

30

31 The spiral separator used in this work was a Walkabout assembly from Mineral Technologies  
32 (Australia). The unit is composed of a four turn Wallaby trough, with a 208 mm pitch and trough  
33 diameter of 360 mm. The sample was fed as a slurry (20 %<sub>w/w</sub> solids) to the top of a spiral, which was  
34 fitted with a funnel (for pulse damping), using a diaphragm pump. At the end of the trough, the  
35 concentrate and tailings were collected separately and analyzed by X-Ray diffraction (XRD), ICP-MS  
36 and quantitative evaluation of minerals by scanning electron microscopy (QEMSCAN). All XRD in this  
37 work was carried out with a Brunker (USA) D8 Discover Diffractometer equipped with a cobalt X-ray  
38 source. Diffraction patterns were analyzed using Xpert High Score software (PANalytical,  
39 Netherlands) to identify the main minerals. Pycnometer measurements were also conducted to  
40 determine the SG of the concentrate. The particle size distribution (Figure A1), SG (Table A1), and  
41 XRD pattern (Figure A2) of the concentrate are shown in Appendix A.  
42  
43  
44  
45  
46  
47  
48  
49  
50

## 51 **2.4 Knelson Concentration**

52

53 The Knelson Concentrator used in this work was a KC MD3 model (FLSmidth Knelson, Canada). It was  
54 operated with a bowl speed of 1250 rpm and fluidizing water rate of 2 L/min. The material was fed  
55 with a flow rate of 250 g/min stopping every 4 min to remove the accumulated concentrate from the  
56 bowl. The particle size distribution, SG (calculated from pycnometer measurements) and major  
57  
58  
59  
60  
61  
62  
63  
64  
65

1 mineral phases (determined by XRD) of the five resultant concentrates were compared to ensure  
2 there were no major differences between concentrates. These results are presented in Appendix A.  
3 The five concentrates were then combined and, along with the tailings fraction, analyzed by ICP-MS  
4 and QEMSCAN.  
5  
6

## 7 **2.5 Chemical Analysis**

8  
9 The REE and zirconium (Zr) content of the feed and products produced from DMS, spiral and Knelson  
10 experiments were determined by ICP-MS. To digest the samples, a homogenous melt was formed by  
11 mixing 0.1 g of sample with sodium peroxide which was then heated. The melt was then digested in  
12 hydrochloric acid. All digestions and ICP-MS analysis in this work were conducted by SGS Canada  
13 (Lakefield, Canada).  
14  
15  
16  
17  
18

## 19 **2.6 Quantitative Evaluation of Minerals by Scanning Electron Microscopy**

20  
21 The products of spiral and Knelson separation experiments, along with a feed sample, were sieved at  
22 150  $\mu\text{m}$ , 106  $\mu\text{m}$ , 75  $\mu\text{m}$  and 53  $\mu\text{m}$ . Representative samples from each size fraction were then  
23 prepared as polished sections and analyzed using QEMSCAN at the Advanced Mineralogy Facility at  
24 SGS Canada (Lakefield, Canada). This technique employs an EVO 430 automated SEM equipped with  
25 four light-element energy-dispersive X-ray spectrometers and iDiscover software for data and image  
26 processing. A reference mineral list was developed using XRD (primarily to define the major  
27 minerals), a SEM equipped with an energy dispersive spectrometer (SEM-EDS), and electron probe  
28 micro analysis (EPMA). REMs were identified based on their major REE composition.  
29  
30  
31  
32  
33  
34  
35

36 The samples were analyzed with the Particle Mineral Analysis (PMA) method. PMA is a two-  
37 dimensional mapping analysis aimed at resolving liberation and locking characteristics of a set of  
38 particles. A pre-defined number of particles were mapped at a pixel size of 3.4 – 7  $\mu\text{m}$ . The typical  
39 diameter of a polished section was 30 mm.  
40  
41  
42  
43

## 44 **2.7 Scanning Electron Microscopy**

45  
46 Representative samples from DMS experiments were prepared as polished sections and analysed  
47 with a Hitachi SU8000 cold field emission SEM (Hitachi High-Technologies, Canada) equipped with an  
48 80 mm<sup>2</sup> X-Max<sup>N</sup> Silicon Drift energy dispersive spectrometer (EDS) detector (Oxford Instruments,  
49 UK). X-ray maps were acquired at an accelerating voltage of 15 kV and beam current of 5  $\mu\text{A}$  for one  
50 hour. The count rate and dead time were approximately 12 kcps and 20 % respectively. The  
51 qualitative phase maps were obtained using AZtec software (Oxford Instruments, UK).  
52  
53  
54  
55  
56  
57  
58  
59  
60  
61  
62  
63  
64  
65

### 3. Results and Discussion

#### 3.1 Feed characteristics

The mineralogy of the feed for gravity separation is shown in Table 1, for each size class. Zircon is significantly concentrated in the + 150  $\mu\text{m}$  and – 75 + 38  $\mu\text{m}$  size fractions. This finding is also demonstrated in the elemental distribution of each size fraction (Table 2), where the concentration of Zr is significantly greater in these same fractions. The concentration of zircon in the – 75 + 38  $\mu\text{m}$  fraction may be due to its grain size distribution in the deposit. The QEMSCAN estimated zircon grain size in the gravity feed is shown in Figure 1. The average grain size is 44  $\mu\text{m}$  and most grains are less than 75  $\mu\text{m}$ . This information, coupled with the findings from previous studies (discussed in Section 1.4), suggest that zircon grains are resistant to grinding and fractures in zircon-bearing particles occur predominantly along the zircon grain boundaries. This would significantly improve the liberation characteristics of zircon allowing for coarser grinds to achieve sufficient liberation. Figure 1 also shows the grain size distribution of REM. Those comprised of predominantly LREE (bastnäsite, synchysite, allanite and monazite) were grouped as LREM and those of HREE [fergusonite and columbite (Fe)] were grouped as HREM. REM (especially HREM) are finely grained in the deposit and would require further grinding for sufficient liberation. It is interesting to note that, like zircon, LREM (such as basnäsite and allanite) are also concentrated in the + 150  $\mu\text{m}$  size fraction (Table 1). This suggests that coarse complex particles containing zircon and LREM in the deposit are more difficult to grind than minerals such as feldspars (K-feldspar and plagioclase), which may provide opportunities for concentration at even coarser particle sizes.



**Table 1 – Mineralogy (in wt %) of the gravity feed (determined by QEMSCAN)**

		Wt %					
	Mineral						
		Combined	+ 150 µm	- 150 + 106 µm	- 106 + 75 µm	- 75 + 53 µm	- 53 + 38 µm
Mass Distribution		100	2.5	7.5	34.1	40.8	15.1
LREM	Bastnäsite	1.1	1.6	1.2	1.1	1.1	1.3
	Synchysite	0.5	0.6	0.4	0.4	0.5	0.6
	Allanite	0.9	1.8	0.9	0.9	0.8	0.9
	Monazite	0.2	0.2	0.1	0.1	0.2	0.3
HREM	Fergusonite	0.1	0.1	0.1	0.1	0.1	0.1
	Columbite (Fe)	0.5	0.6	0.4	0.4	0.5	0.6
	Zircon	6.2	7.2	4.1	4.9	6.6	9.4
Silicate Gangue	Quartz	15.4	19.4	16.5	16.1	15.1	13.7
	K-Feldspar	25.8	19.5	29.5	27.4	25.6	21.7
	Plagioclase	28.5	20.1	29.4	30.0	28.6	25.4
	Biotite	7.1	8.3	6.8	6.8	7.2	7.2
Other Gangue	Fe – Oxides	8.0	13.0	5.5	6.1	7.9	12.6
	Other	5.7	7.6	5.0	5.6	5.8	6.0

**Table 2 – Concentration (in wt %) of valuable elements in the gravity feed (determined by ICP-MS)**

		Wt %					
Metals							
		Combined	+ 150 µm	- 150 + 106 µm	- 106 + 75 µm	- 75 + 53 µm	- 53 + 38 µm
Mass Distribution		100	2.5	7.5	34.1	40.8	15.1
Zr		2.5	2.8	1.8	1.9	2.7	3.5
LREE		1.0	1.3	0.9	0.9	1.0	1.4
HREE		0.2	0.3	0.2	0.2	0.2	0.3

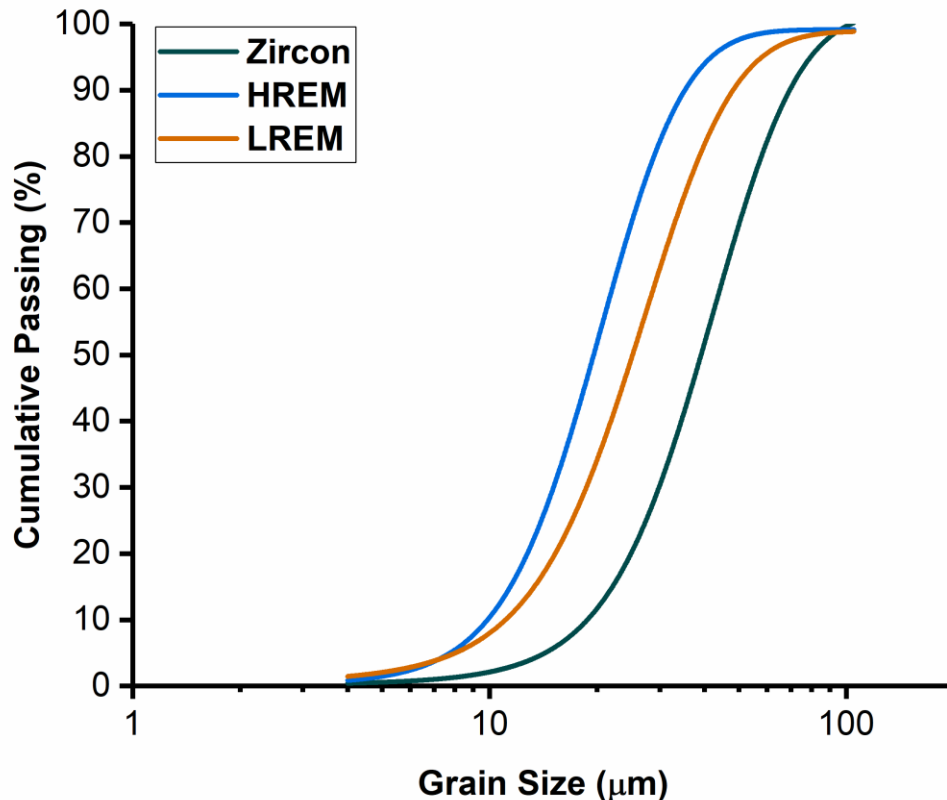


**Figure 1 – Grain size distribution of zircon, HREM [fergusonite + columbite (Fe)] and LREM (bastnäsite + synchysite + allanite + monazite) estimated by QEMSCAN**

Liberation and association characteristics for all major mineral classes in the deposit are shown in Figure 2. Mineral particles were grouped into free, liberated, binary and complex. Minerals having > 95 % of the particle surface area are referred to as “free”, and those with < 95 % and > 80 % of the particle surface area are considered “liberated”. Across all particle sizes, liberation (free + liberated) of zircon is 59 % with 44 % of the particles being free zircon. Slightly over 50 % of the zircon grains are > 38 μm in the gravity feed (Figure 1) suggesting that most of these grains are liberated. Although a more detailed study is required to investigate the comminution properties of the ore, the present results further reinforce the notion that fractures in particles containing zircon occur preferentially at grain boundaries, rather than through zircon grains. Figures 2b and 2c show the association characteristics of HREM and LREM, respectively, indicating that further grinding is required to liberate them. The liberation characteristics of the major gangue minerals in the deposit (Fe oxides, quartz and feldspars) are shown in Figures 2d to 2f. Quartz and feldspars are well liberated (> 70 %), and Fe oxides are approximately 50 % liberated. Fe oxides are expected to be recovered in the gravity pre-concentrate, and therefore, would need to be removed with a downstream process (*e.g.* magnetic separation).

Mineral particles in the feed can be grouped into different SG classes using the QEMSCAN data. This is done by assigning each mineral a SG value and then calculating the SG of each particle as a function of its constituents. Thus, upgrade ratio and recovery plots for each mineral can be produced by artificially splitting the sample at the desired SG. Figure 3 shows the data for value minerals (zircon, LREM and HREM) split at a SG of 2.75, 2.95 and 3.5. This analysis indicates that splitting the feed at a SG of 2.75 results in the recovery of > 95 % of value minerals with upgrade ratios above 2.7. Increasing the SG to 2.95 offers an improvement in upgrading (zircon: 3.2; HREM: 3.1; LREM: 3.2) with minimal reduction in recovery (zircon: 92 %; HREM: 88 %; LREM: 92 %). This suggests that only a small number of valuable mineral-bearing particles have a SG < 2.95. An additional increase to a SG of 3.5, QEMSCAN predicts recoveries of 75 % zircon, 72 % HREM and 68 % LREM, with upgrade ratios of 4.8, 4.6 and 4.4, respectively. The high proportion of zircon-bearing particles with SG > 3.5 corresponds well to its liberation characteristics (Figure 2a). However, as REM are fine-grained (Figure 1) and poorly liberated (Figure 2b and 2c), it is expected that a much lower proportion of these minerals be present as high SG particles. This suggests that mineral associations (relatively high SG minerals associated with each other in complex particles) may provide opportunities to effectively recover both zircon- and REM-bearing particles by gravity separation, even without complete liberation.

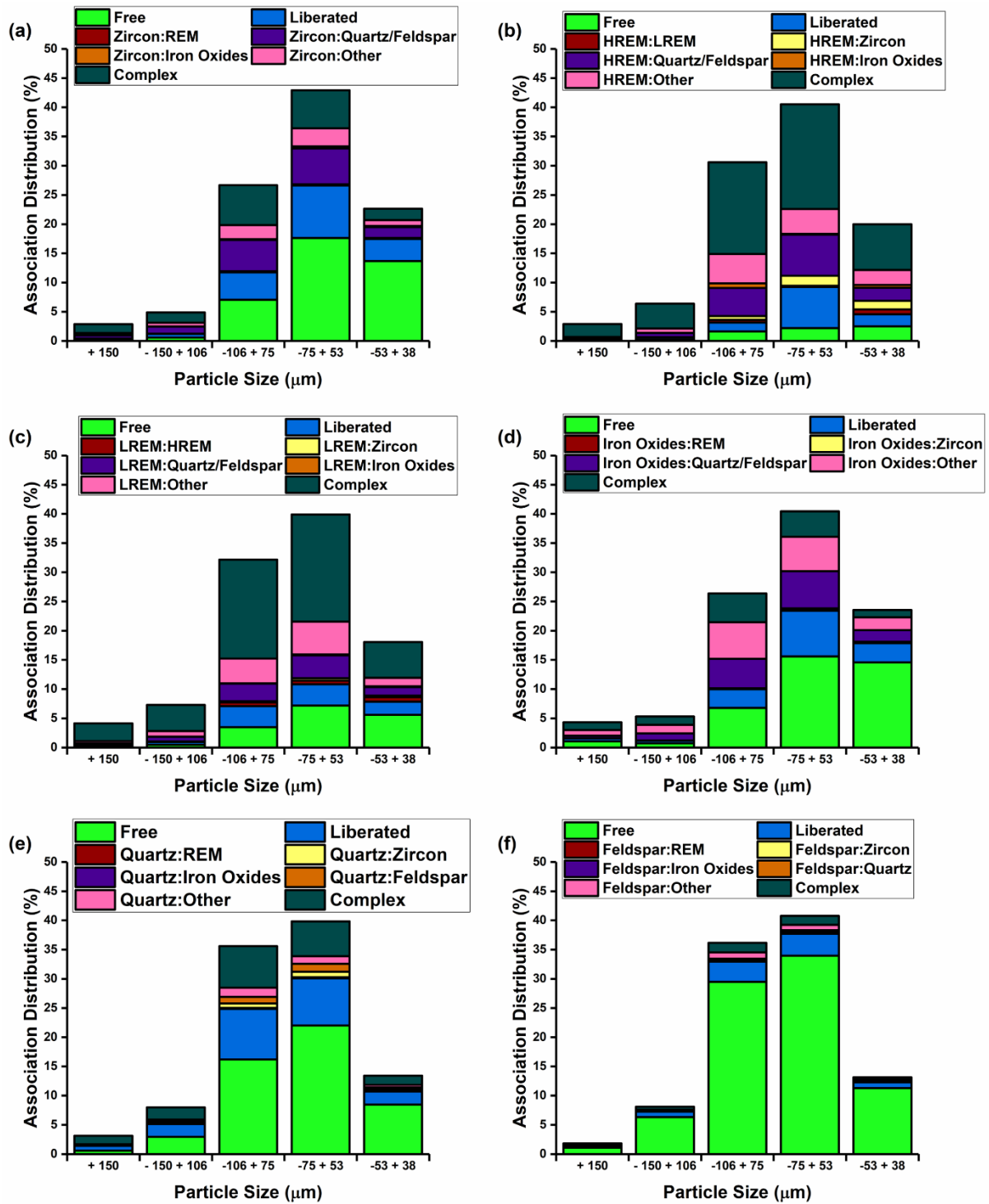
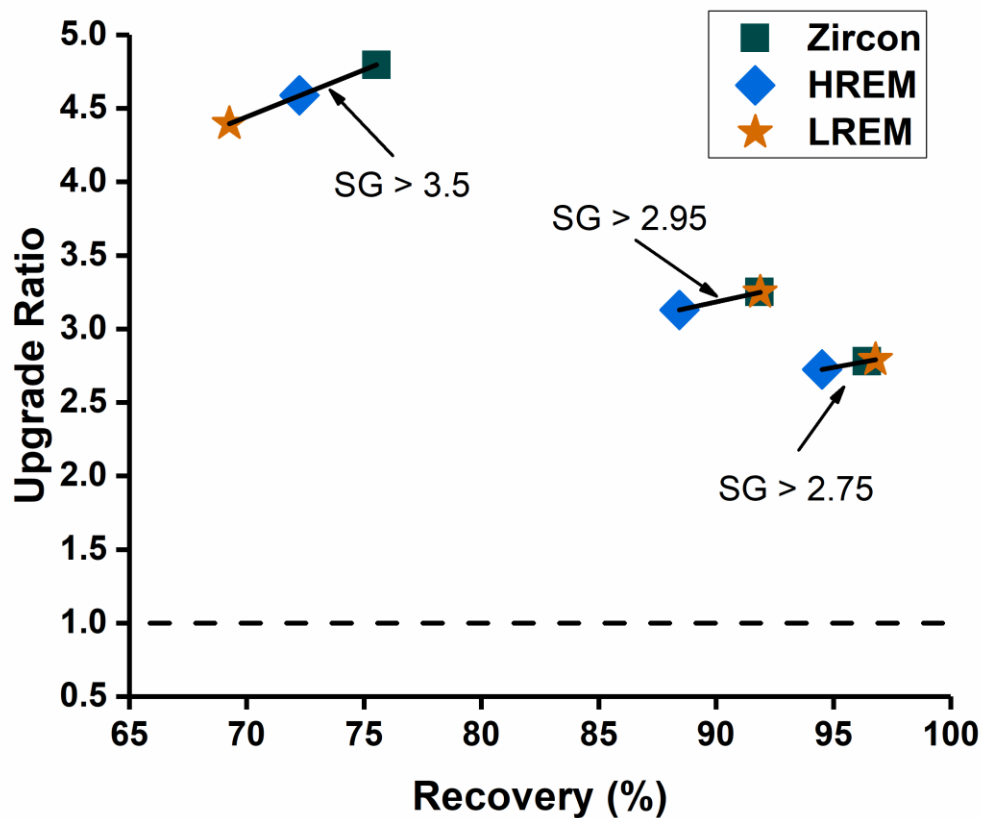


Figure 2 – Mineral associations by particle size in the gravity feed for (a) zircon, (b) HREM, (c) LREM, (d) Fe oxides, (e) quartz and (f) feldspars



**Figure 3 – Upgrade ratio and recovery of zircon, HREM and LREM by SG, predicted by QEMSCAN**

### 3.2 Dense Medium Separation

Figure 4 shows the upgrade ratio of Zr, LREE and HREE in the DMS sink fractions when using a heavy liquid with a SG of 2.95 and 2.75. The results indicate that 81 % of Zr and 76 % of REE can be recovered, with upgrade ratios of 4.2 and 3.9 respectively, when processing the material using a heavy liquid with a SG of 2.95. Zr and REE recoveries were increased to 95 % and 92 %, respectively, at a SG of 2.75. However, upgrading was impacted (Zr: 2.9; REE: 2.8), due to the recovery of less liberated material. These results are in good agreement with the mineralogical upgrading and recovery determined by QEMSCAN analysis on the feed sample (Figure 3). This demonstrates gravity modeling using QEMSCAN can be used confidently, to predict grade and recovery values by SG for DMS.

SEM-EDS was used to identify Zr, Fe, cerium (Ce) and Y in the sink and float fractions at a SG of 2.75 (Figure 5). While only qualitative, the SEM images provide an empirical check for the conclusions drawn from QEMSCAN (Section 3.1), which assigns mineral chemistry based on a definition data

base. This analysis clearly shows valuable minerals (and Fe oxides) are concentrated in the DMS sink fraction. Zircon is recovered as both coarse liberated particles and fine-grained material which remains locked with other minerals in the feed. The SEM images show Y alongside Zr, demonstrating the importance of recovering zircon for the recovery of HREE. Minerals bearing LREE, such as Ce, are generally finely grained and poorly liberated. However, they are found in particles containing other REM, zircon and/or Fe oxide grains, confirming that mineral association characteristics provide opportunities for the recovery of less liberated material. Although DMS represents near ideal gravity separation and the upgrade ratios obtained here are likely not possible using conventional or enhanced gravity concentrators, the results indicate that gravity separation may be effective at selectively recovering both zircon and REM.

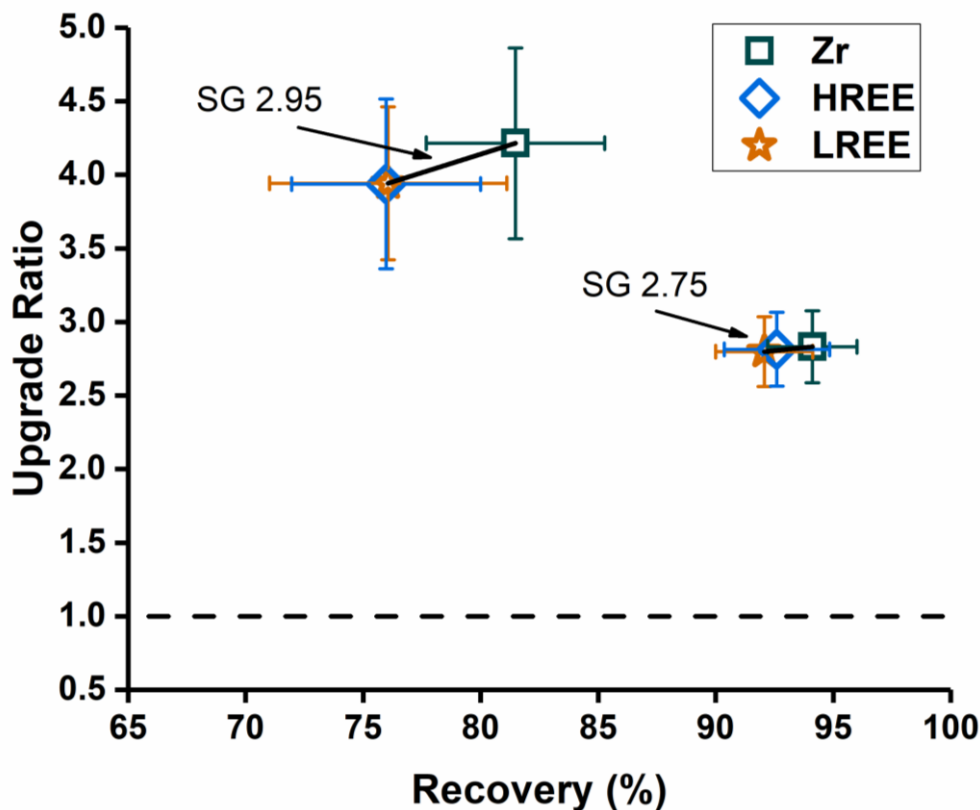
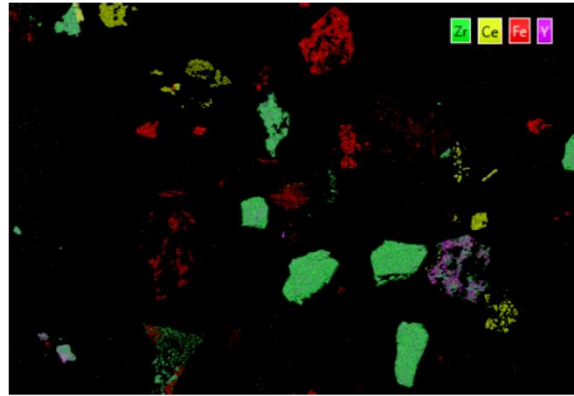
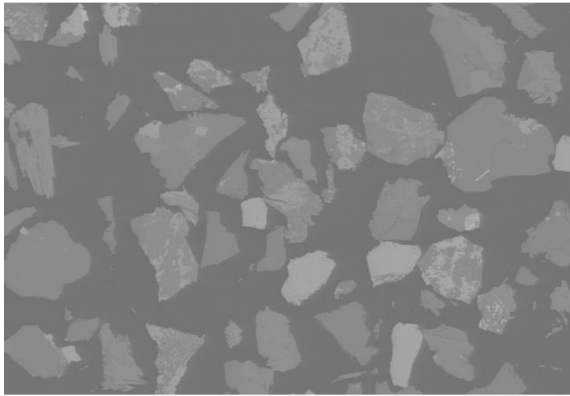


**Figure 4 – Upgrade ratio and recovery of valuable elements from DMS sink fractions with a heavy liquid of SG 2.95 and 2.75 (Error bars represent 95 % confidence intervals)**

### Sink



### Float

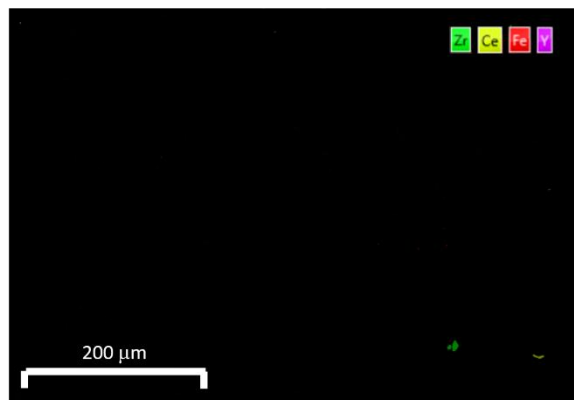


**Figure 5 – BSE image (left) and elemental (Zr, Ce, Fe, Y) phase identification (right) of the DMS sink and float fraction produced using a heavy liquid with a SG of 2.75**

### **3.3 Spiral Concentrator**

Plots of the upgrade ratio vs recovery for the major mineral classes and valuable elements in the spiral concentrate are shown in Figures 6 and 7, respectively. The results indicate that all relatively high SG minerals (zircon, Fe oxides and REM) in the deposit are concentrated, while the gangue minerals (predominately feldspars) are rejected. The spiral concentrator was most effective at upgrading zircon, with an upgrade ratio of 2.0, followed by Fe oxides (1.9), LREM (1.6) and then HREM (1.4). Elemental upgrade ratios for Zr, LREE and HREE were 1.7, 1.8 and 1.7 respectively. The minor discrepancies between chemical assays and QEMSCAN results (most notably between Zr and zircon) are likely caused by differential settling and density segregation of particles during preparation of the polished sections. This is a common concern when creating polished sections for QEMSCAN (Coetzee *et al.*, 2011; Kwitko-Ribeiro, 2012; Speirs *et al.*, 2008); and in this case, results in small overestimations of zircon. Although the recoveries of relatively high SG minerals in the deposit are low, examining the mineral liberation and association characteristics of the spiral concentrate and tailings (Figure 8), suggests that zircon and Fe oxide recoveries are likely low due to the lack of

recirculation, rather than insufficient liberation. The findings from Section 3.1 and 3.2 may also suggest that further processing through multiple spiral concentrators may also improve the recovery of REM.

Although quartz is relatively well liberated, it is not well rejected by the spiral concentrator. Figure 9 suggests that particle size has a large impact on quartz recovery. The spiral concentrator can reject fine ( $< 75 \mu\text{m}$ ) quartz particles, but, coarse ( $> 75 \mu\text{m}$ ) quartz-bearing particles tend to be concentrated by the spiral. Figure 9 indicates that, in general, the spiral concentrator is preferentially recovering coarse particles in the feed. Minimal upgrading is obtainable at particle sizes greater than  $150 \mu\text{m}$ , but, the spiral concentrator is effective at upgrading the high SG minerals in the finer size fractions. Zircon and REM, in the  $-150 + 106 \mu\text{m}$  fraction, are effectively upgraded and recovered, even though they are poorly liberated (Figure 2a-d). This implies grain size differences and mineral associations allow for the effective separation of coarse unliberated valuable material, but only at particle size ranges less than  $150 \mu\text{m}$ .

Figure 10 shows the recovery of zircon and LREM by SG class at each particle size. It can be noted that the spiral concentrator is favouring the recovery of particles with more elevated SG across all size ranges for both zircon and LREM, except for the  $+150 \mu\text{m}$  size fraction, reinforcing that the spiral may only be applicable for this deposit at finer ( $< 150 \mu\text{m}$ ) particle sizes. It is important to note that the spiral and operating conditions (pulp density, flow rate, *etc.*) used for this study have not been optimized. Thus, the use of a spiral concentrator better suited for fine particle separation ( $< 100 \mu\text{m}$ ) and through further optimization, significant improvements could be observed.



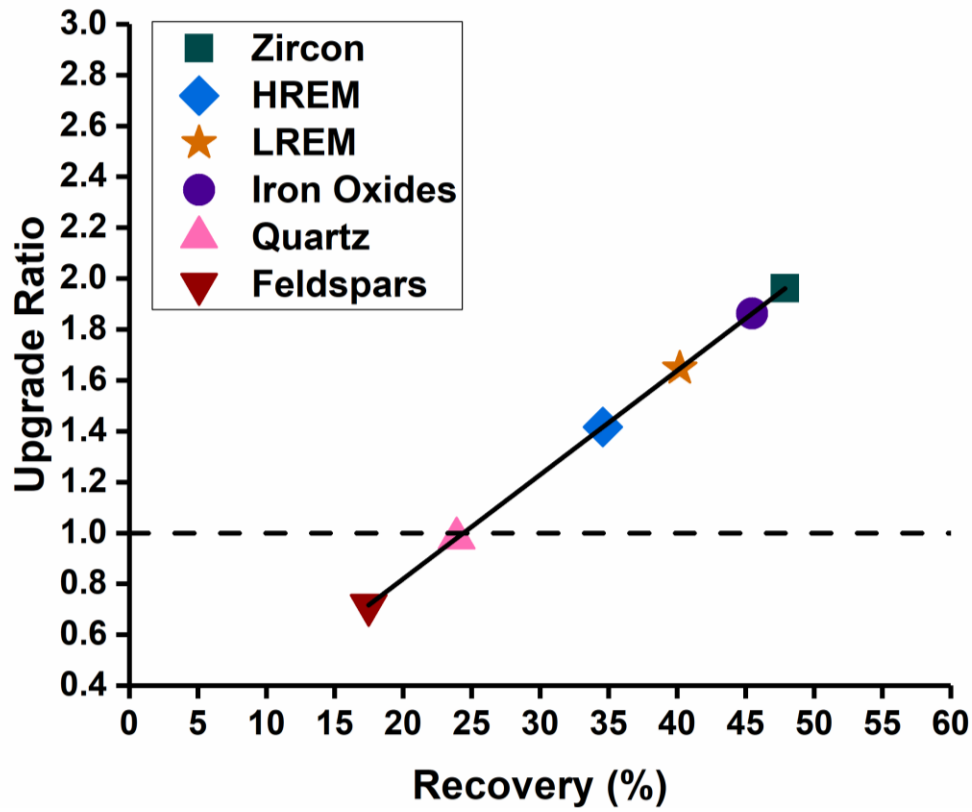


Figure 6 – Upgrade ratio and recovery of the major mineral classes in the spiral concentrate

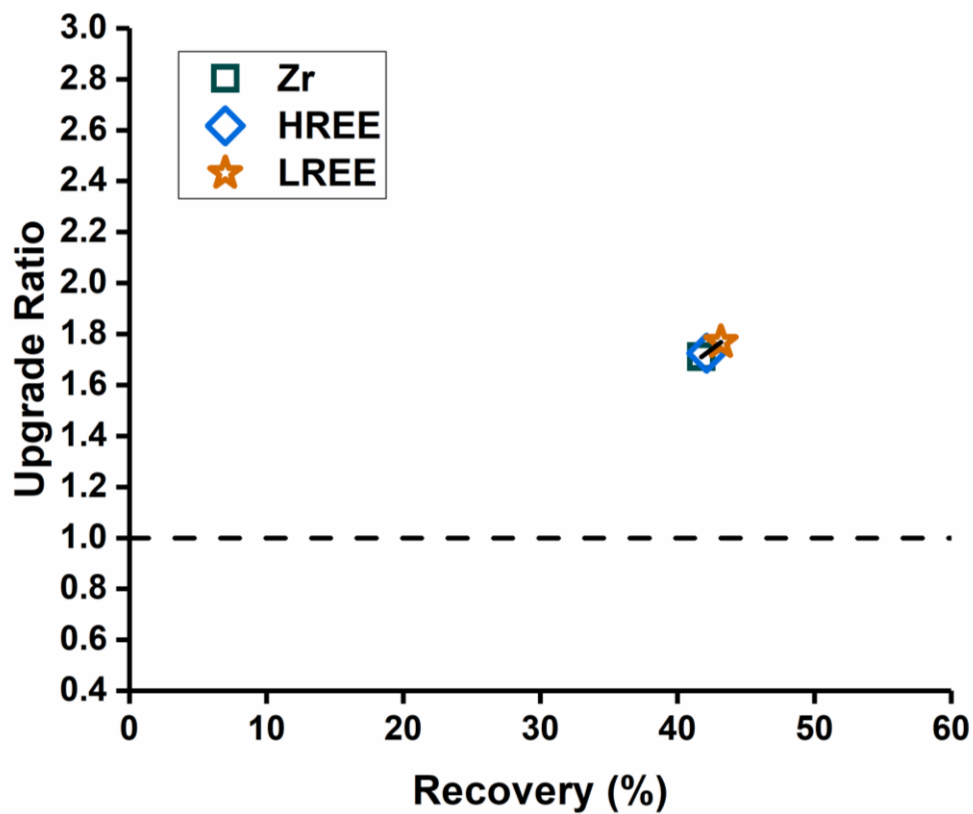


Figure 7 – Upgrade ratio and recovery of valuable elements in the spiral concentrate

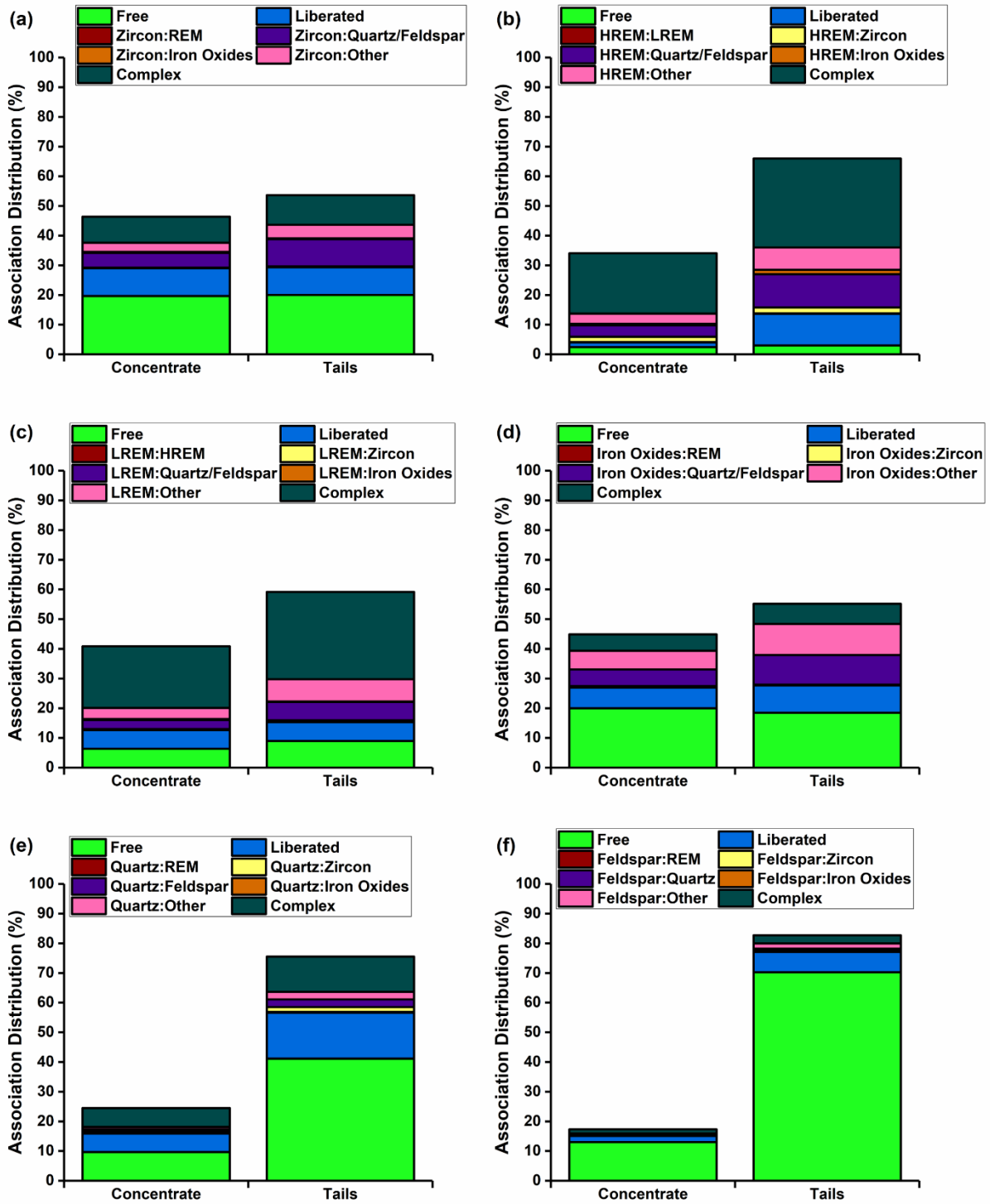


Figure 8– Mineral associations of the spiral products for (a) zircon, (b) HREM, (c) LREM, (d) Fe oxides, (e) quartz and (d) feldspars

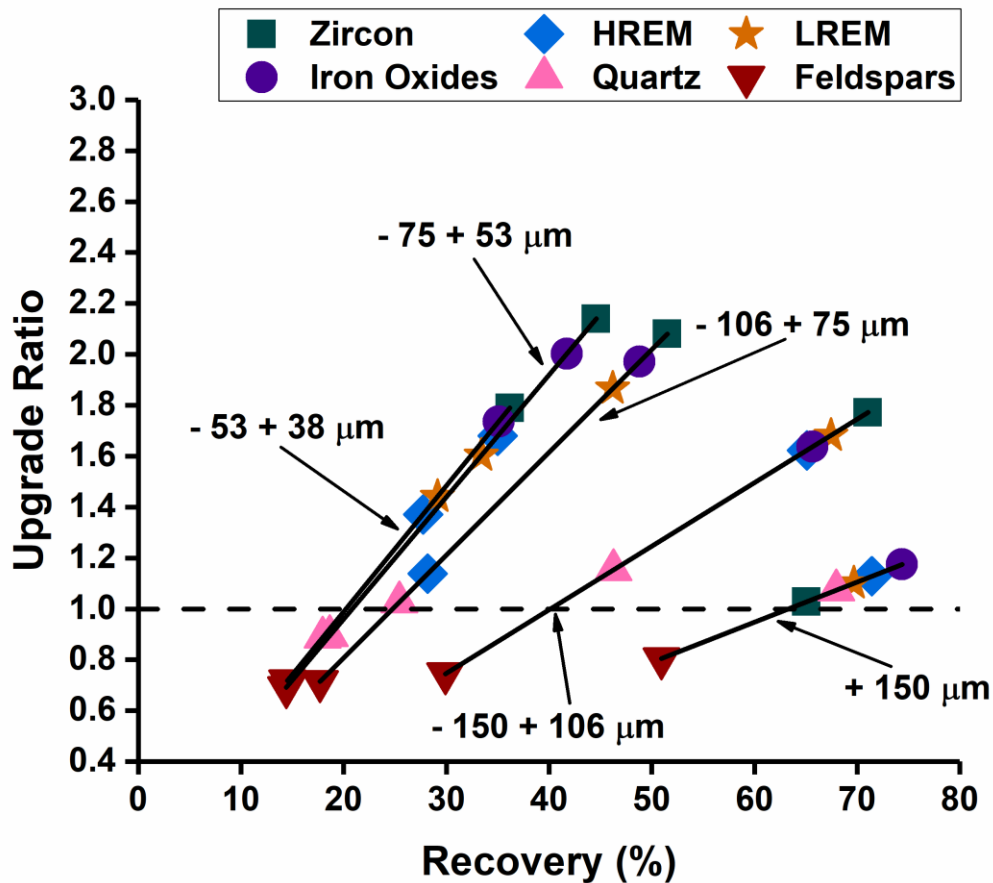


Figure 9 – Upgrade ratio and recovery of the major mineral classes in the spiral concentrate sorted by size

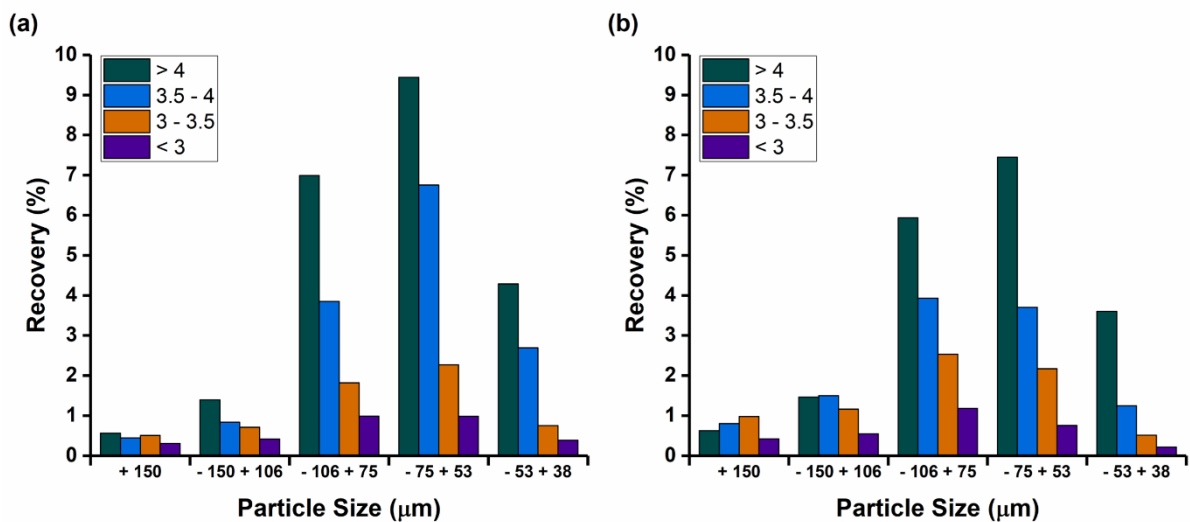


Figure 10 – Recovery of the spiral concentrator sorted by SG for particles containing (a) zircon and (b) LREM across each size class

### 3.3 Knelson Concentrator

An analysis, like that performed on the spiral products, was conducted on the Knelson concentrate and tailings. Figure 11 shows the upgrade ratio vs. recovery for the major mineral classes in the deposit; Figure 12 the upgrade ratio vs. recovery of valuable elements; Figure 13 the mineral liberation and association data; Figure 14 the size by size upgrading and recovery of each mineral class; and Figure 15 the recovery of zircon and LREM by SG class. The Knelson concentrator provides better selectivity over the spiral concentrator, with improved quartz and feldspar rejection. The largest improvement in selectivity was for Fe oxides, which increases from an upgrade ratio of 1.9 with the spiral to 2.6 with the Knelson Concentrator. Improved upgrading of the value minerals was also observed (zircon: 2.0 to 2.3, HREM: 1.4 to 1.8, LREM: 1.5 to 2.1). The liberation and association data for the Knelson products (Figure 13), compared to those obtained for the spiral products (Figure 8), suggest that the Knelson concentrator yields improved upgrading through both better rejection of liberated gangue and selectivity for liberated high SG zircon- and LREM-bearing particles (Figure 15). The ability to better reject liberated gangue is partially attributed to the fact that particle size is a minor factor in separation (Figure 14). Particles > 150  $\mu\text{m}$  continued to be preferentially recovered, but there remains upgrading of value minerals in this size fraction. Thus, the use of a centrifugal gravity separator, such as a Knelson Concentrator, may provide opportunities for processing this deposit at coarser size fractions than a spiral concentrator. Similar to the spiral results, the lack of recirculation is the likely cause for poor mineral recoveries and through optimization further improvements might be observed.

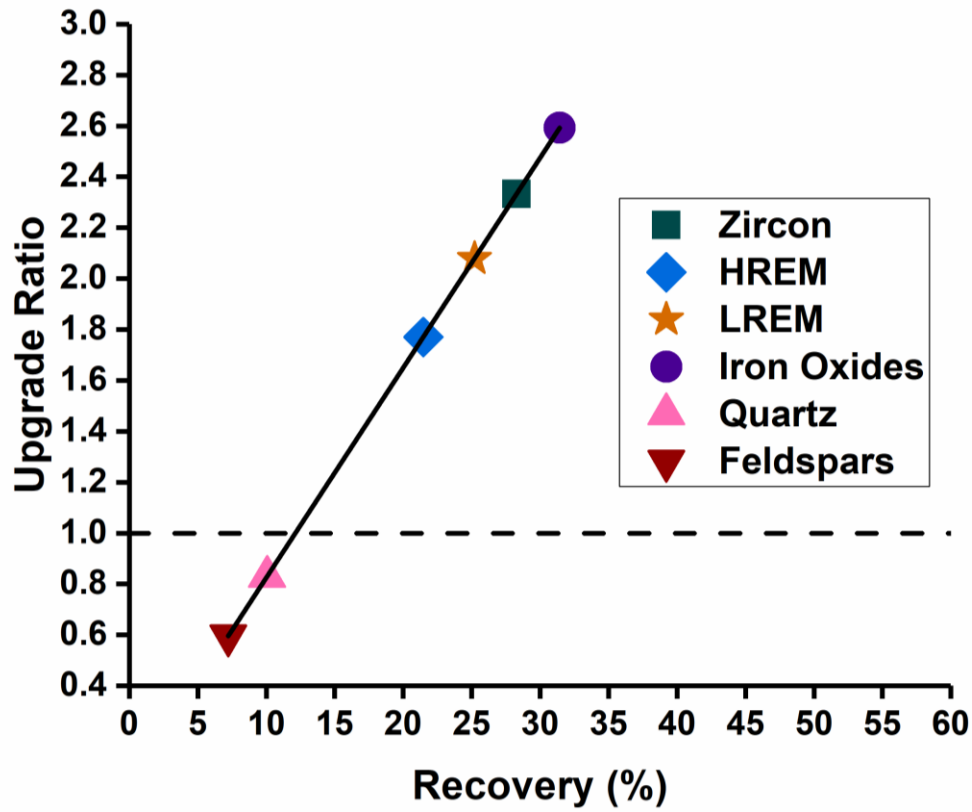


Figure 11 – Upgrade ratio and recovery of the major mineral classes in the Knelson concentrate

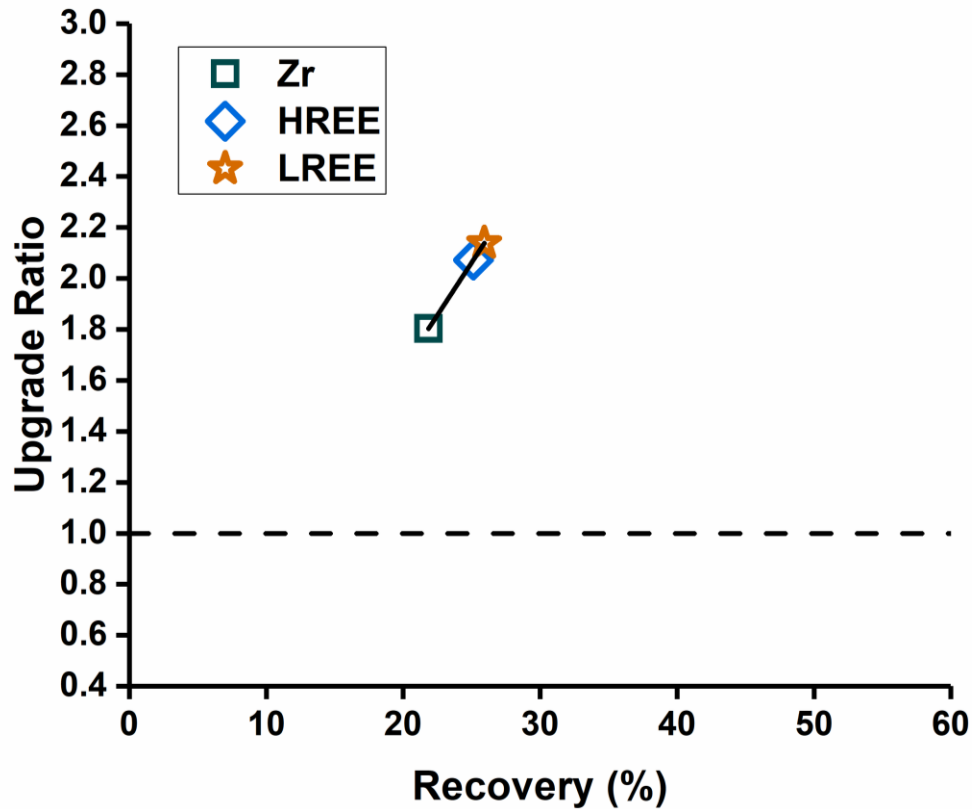


Figure 12 – Upgrade ratio and recovery of valuable elements in the Knelson concentrate

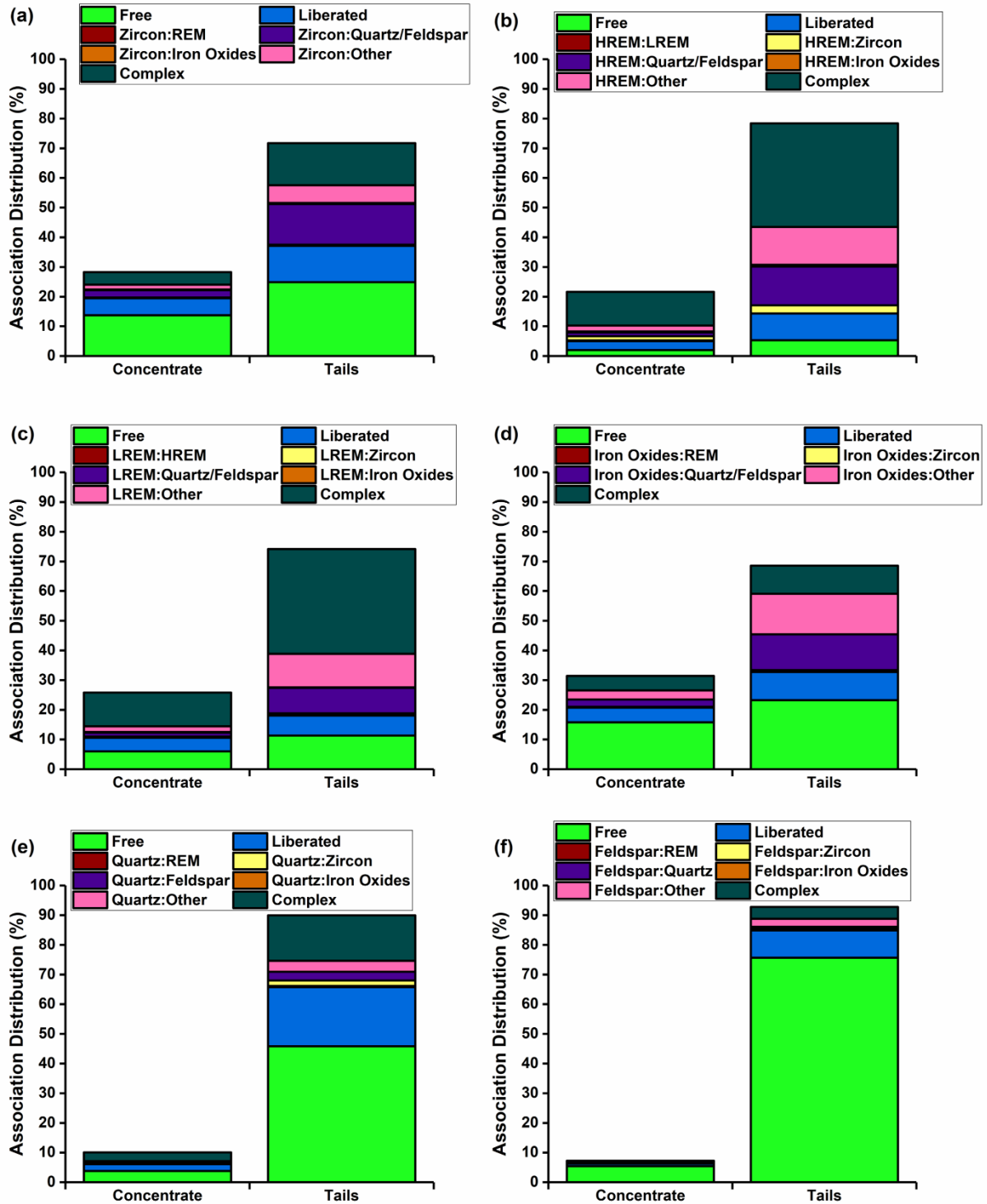


Figure 13 – Mineral associations of the Knelson products for (a) zircon, (b) HREM, (c) LREM, (d) Fe oxides, (e) quartz and (d) feldspars

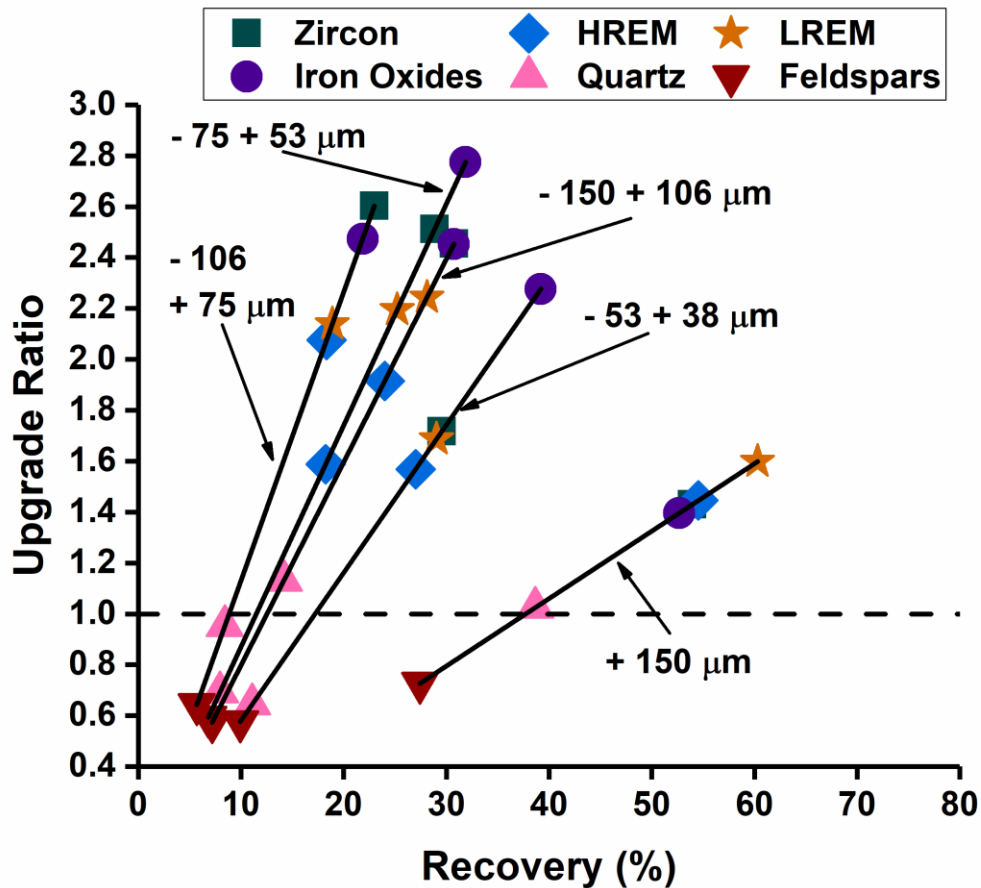


Figure 14 – Upgrade ratio and recovery of the major mineral classes in the Knelson concentrate sorted by size

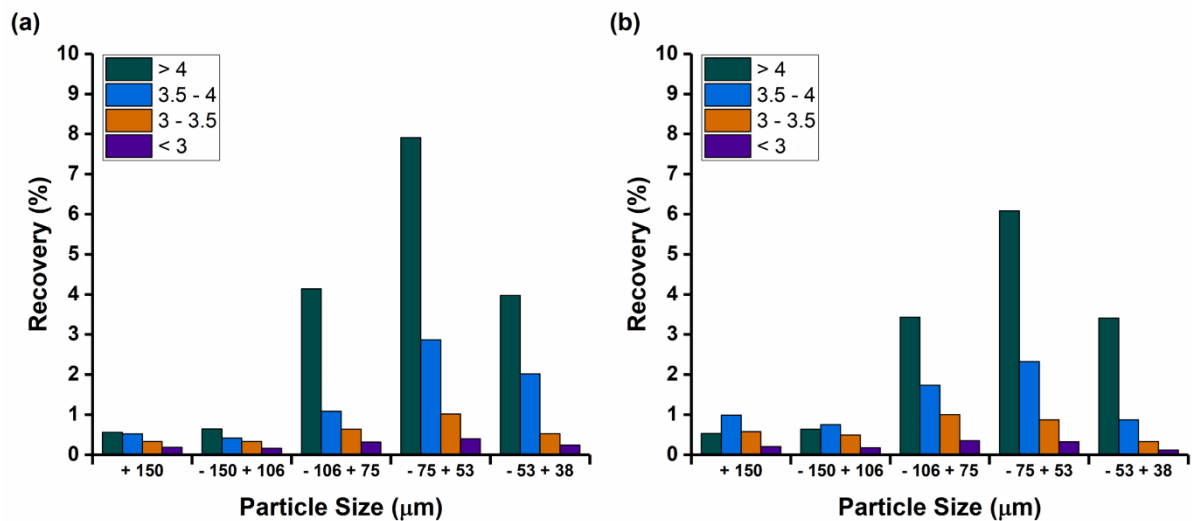


Figure 15 – Recovery of the Knelson Concentrator sorted by SG for particles containing (a) zircon and (b) LREM across each size class

## Conclusions

This study investigated the use of a spiral concentrator and a Knelson Concentrator as a pre-concentration step for a coarse Nechalacho feed. ICP-MS was used to determine the content of valuable elements in gravity products and QEMSCAN to identify how particle size, mineral liberation and association characteristics, and mineral particle SG distributions affect each gravity technique.

The conclusions are as follows:

1. DMS results were accurately predicted by QEMSCAN gravity modeling of the feed.
2. QEMSCAN gravity modeling and DMS experiments indicate that mineral grain size differences and association characteristics provide opportunities to pre-concentrate the Nechalacho deposit at relatively coarse particle sizes using gravity separation.
3. Both the spiral concentrator and the Knelson Concentrator were effective at pre-concentrating the material, achieving zircon upgrade ratios of 2.0 and 2.3, respectively. Both processes reject predominately feldspar gangue and fine quartz particles.
4. Particle size had a significant effect when using the spiral, but much less so for the Knelson Concentrator. The spiral preferentially recovered coarser particles, whereas the Knelson showed little bias between particles sizes.
5. The spiral concentrator was only effective in the -150  $\mu\text{m}$  particle range, whereas, the Knelson Concentrator remained effective at coarser sizes; suggesting opportunities for even coarser grinds when using centrifugal separators.

## Acknowledgements

The authors would like to acknowledge the Natural Sciences and Engineering Research Council of Canada (NSERC) and Avalon Advanced Materials Inc. for providing funding for this work through the Collaborative Research and Development (CRD) Program (CRDPJ 44537-12). C. Marion and S. Rudinsky would also like to acknowledge funding from the McGill Engineering Doctoral Award and the NSERC Alexander Graham Bell Canada Graduate Scholarships Program. The authors would also like to thank the Advanced Mineralogy Facility at SGS Canada (Lakefield) for the ICP-MS and QEMSCAN analysis.



## References

- Browning, J.S., 1961. Heavy Liquids and Procedures for Laboratory Separation of Minerals. U.S. Bureau of Mines.
- Ciuculescu, T., Foo, B., Gowans, R., Hawton, K., Jacobs, C., Spooner, J., 2013. Technical Report Disclosing the Results of the Feasibility Study on the Nechalacho Rare Earth Elements Project. Avalon Rare Metals Inc.
- Coetzee, L.L., Theron, S.J., Martin, G.J., Merwe, J.-D.v.d., Stanek, T.A., 2011. Modern Gold Departments and Its Application to Industry. Minerals Engineering 24, 565-575.
- Golev, A., Scott, M., Erskine, P.D., Ali, S.H., Ballantyne, G.R., 2014. Rare Earths Supply Chains: Current Status, Constraints and Opportunities. Resources Policy 41, 52-59.
- Grammatikopoulos, T., Mercer, W., Gunning, C., Prout, S., 2011. Quantitative Characterization of the Ree Minerals by Qemscan from the Nechalacho Heavy Rare Earth Deposit, Thor Lake Project, Nwt, Canada, 43rd Annual Meeting of the Canadian Mineral Processors, Ottawa, Canada.
- Gupta, C.K., Krishnamurthy, N., 2005. Extractive Metallurgy of Rare Earths. CRC press, Boca Raton, Florida.
- Jordens, A., Cheng, Y.P., Waters, K.E., 2013. A Review of the Beneficiation of Rare Earth Element Bearing Minerals. Minerals Engineering 41, 97-114.
- Jordens, A., Marion, C., Grammatikopoulos, T., Hart, B., Waters, K.E., 2016a. Beneficiation of the Nechalacho Rare Earth Deposit: Flotation Response Using Benzohydroxamic Acid. Minerals Engineering 99, 158-169.
- Jordens, A., Marion, C., Langlois, R., Grammatikopoulos, T., Rowson, N.A., Waters, K.E., 2016b. Beneficiation of the Nechalacho Rare Earth Deposit. Part 1: Gravity and Magnetic Separation. Minerals Engineering 99, 111-122.
- Jordens, A., Marion, C., Langlois, R., Grammatikopoulos, T., Sheridan, R.S., Teng, C., Demers, H., Gauvin, R., Rowson, N.A., Waters, K.E., 2016c. Beneficiation of the Nechalacho Rare Earth Deposit. Part 2: Characterisation of Products from Gravity and Magnetic Separation. Minerals Engineering 99, 96-110.
- Jordens, A., Sheridan, R.S., Rowson, N.A., Waters, K.E., 2014. Processing a Rare Earth Mineral Deposit Using Gravity and Magnetic Separation. Minerals Engineering 62, 9-18.

Kwitko-Ribeiro, R., 2012. New Sample Preparation Developments to Minimize Mineral Segregation in Process Mineralogy, in: Broekmans, M.A.T.M. (Ed.), Proceedings of the 10th International Congress for Applied Mineralogy (Icam). Springer Berlin Heidelberg, Berlin, Heidelberg, pp. 411-417.

Napier-Munn, T.J., Bosman, J., Holtham, P.N., 2014. Innovations in Dense Medium Separation Technology, in: Anderson, C.G., Dunne, R.C., Uhrig, J.L. (Eds.), Mineral Processing and Extractive Metallurgy: 100 Years of Innovation. Society for Mining Metallurgy & Exploration, Englewood, United States, pp. 265-275.

Paulick, H., Machacek, E., 2017. The Global Rare Earth Element Exploration Boom: An Analysis of Resources Outside of China and Discussion of Development Perspectives. Resources Policy 52, 134-153.

Richards, R.G., MacHunter, D.M., Gates, P.J., Palmer, M.K., 2000. Gravity Separation of Ultra-Fine (<0.1mm) Minerals Using Spiral Separators. Minerals Engineering 13, 65-77.

Seredin, V.V., 2010. A New Method for Primary Evaluation of the Outlook for Rare Earth Element Ores. Geology of Ore Deposits 52, 428-433.

Speirs, J.C., McGowan, H.A., Neil, D.T., 2008. Polar Eolian Sand Transport: Grain Characteristics Determined by an Automated Scanning Electron Microscope (Qemscan®). Arctic, Antarctic, and Alpine Research 40, 731-743.

U.S. Department of Energy, 2011. Critical Materials Strategy. U.S. Department of Energy.

Weng, Z., Jowitt, S.M., Mudd, G.M., Haque, N., 2015. A Detailed Assessment of Global Rare Earth Element Resources: Opportunities and Challenges. Economic Geology 110, 1925-1952.

Wills, B.A., Finch, J.A., 2016a. Chapter 10 - Gravity Concentration, Wills' Mineral Processing Technology (Eighth Edition). Butterworth-Heinemann, Boston, pp. 223-244.

Wills, B.A., Finch, J.A., 2016b. Chapter 11 - Dense Medium Separation, Wills' Mineral Processing Technology (Eighth Edition). Butterworth-Heinemann, Boston, pp. 245-264.

Xia, L., Hart, B., Douglas, K., 2015a. The Role of Citric Acid in the Flotation Separation of Rare Earth from the Silicates. Minerals Engineering 74, 123-129.

Xia, L., Hart, B., Loshusan, B., 2015b. A ToF-SIMS Analysis of the Effect of Lead Nitrate on Rare Earth Flotation. Minerals Engineering 70, 119-129.

Zhang, J., Edwards, C., 2012. A Review of Rare Earth Mineral Processing Technology, 44th Annual Meeting of The Canadian Mineral Processors, Ottawa, Canada.

## Appendix A

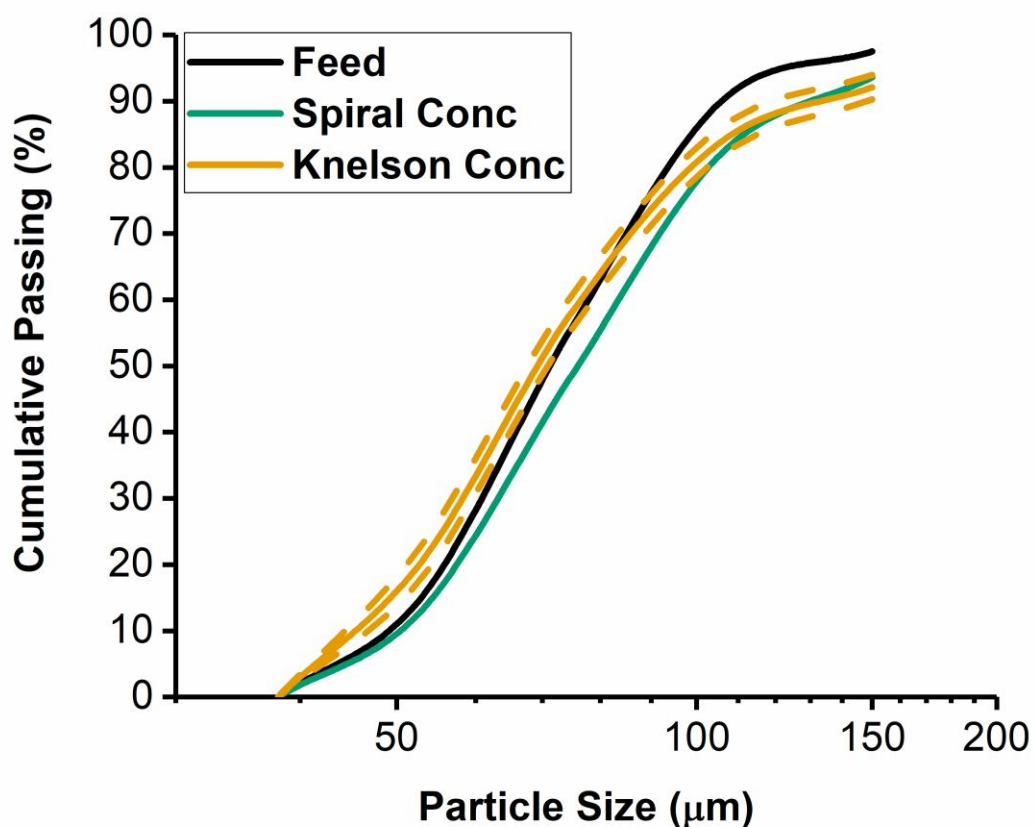


Figure A1 – Particle size distribution of the gravity feed, spiral concentrate and Knelson concentrate. The distribution shown for the Knelson concentrate is the average of the five concentrates with the dashed line representing the 95 % confidence interval

Table A1 – Mass recovery and SG (calculated from pycnometer measurements) of the spiral and Knelson Concentrates. Data for the Knelson concentrate is respective to each 4-min interval during which concentrate was collected, where mass recovery and SG are the average of the 5 concentrates produced

Sample	Mass Recovery (%)	95 % Confidence	SG	95 % Confidence
Feed	-	-	2.6	-
Spiral Conc	24.4	-	2.9	-
Knelson Conc	12.1	0.4	3.1	0.1

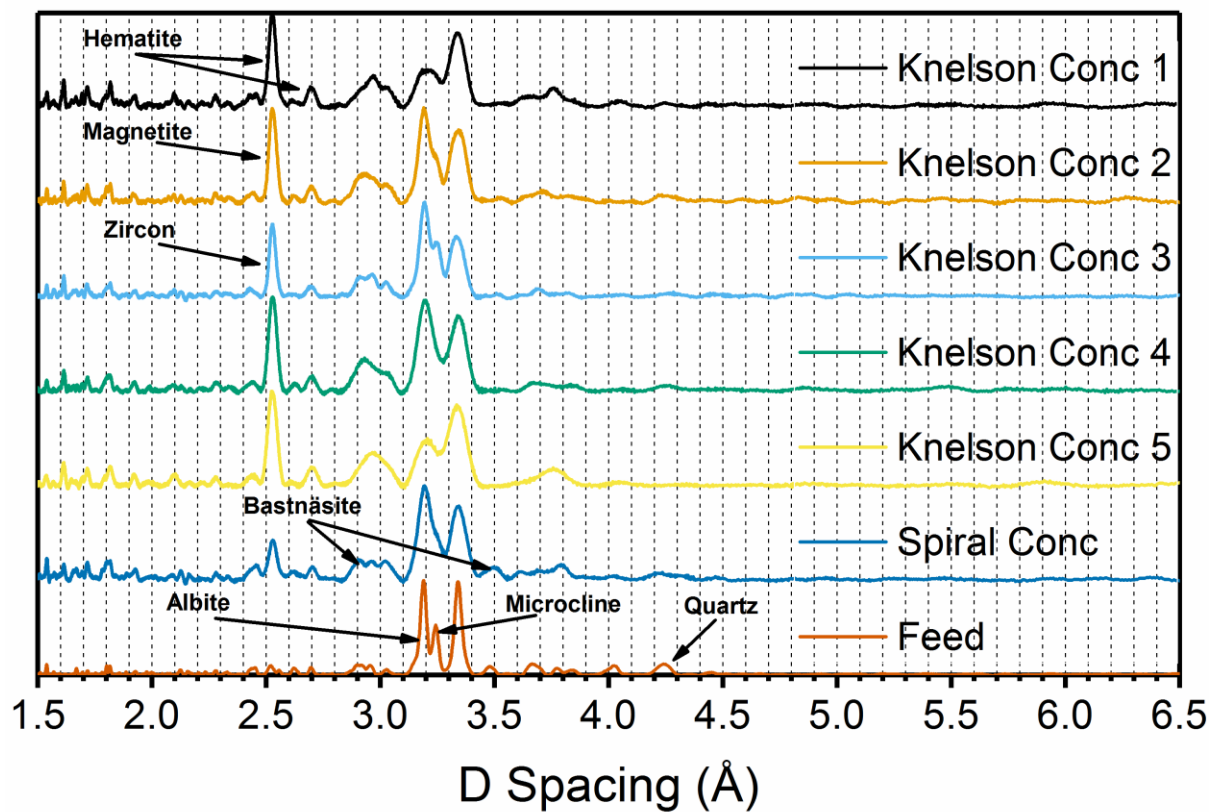
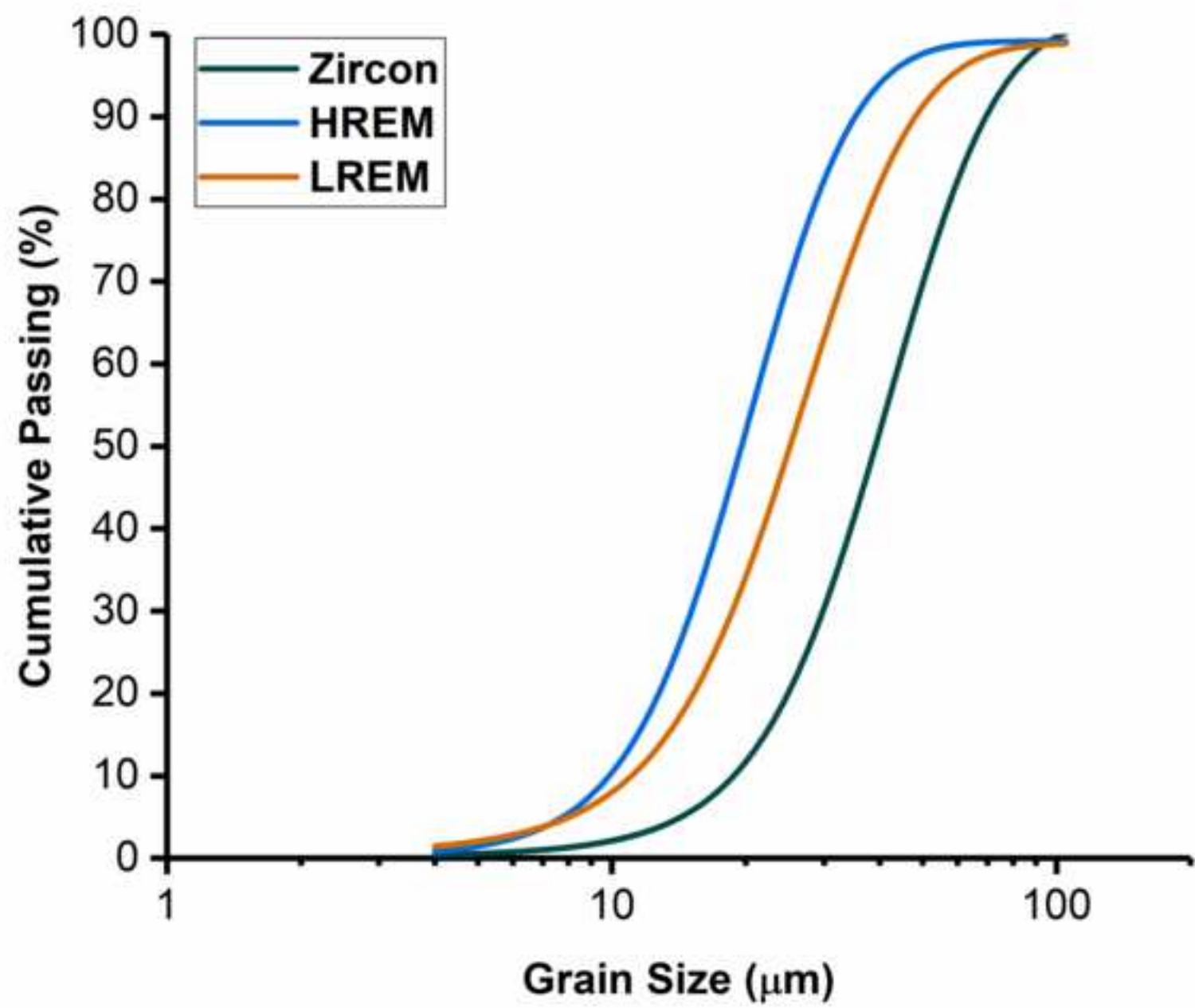


Figure A2 – XRD results for the five Knelson concentrates, the spiral concentrate and the feed sample

Figure 1  
[Click here to download high resolution image](#)



**Figure 2**  
[Click here to download high resolution image](#)

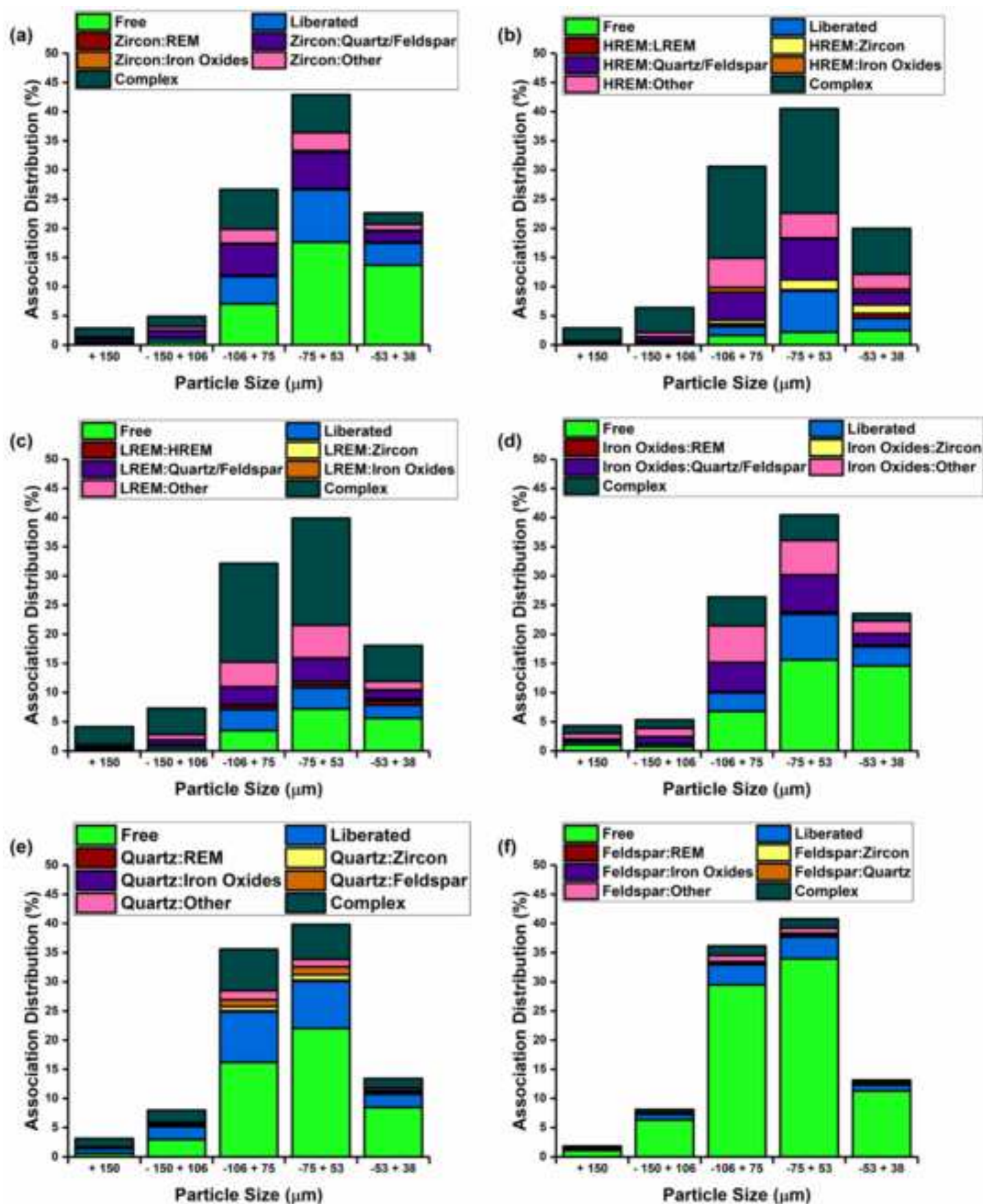


Figure 3  
[Click here to download high resolution image](#)

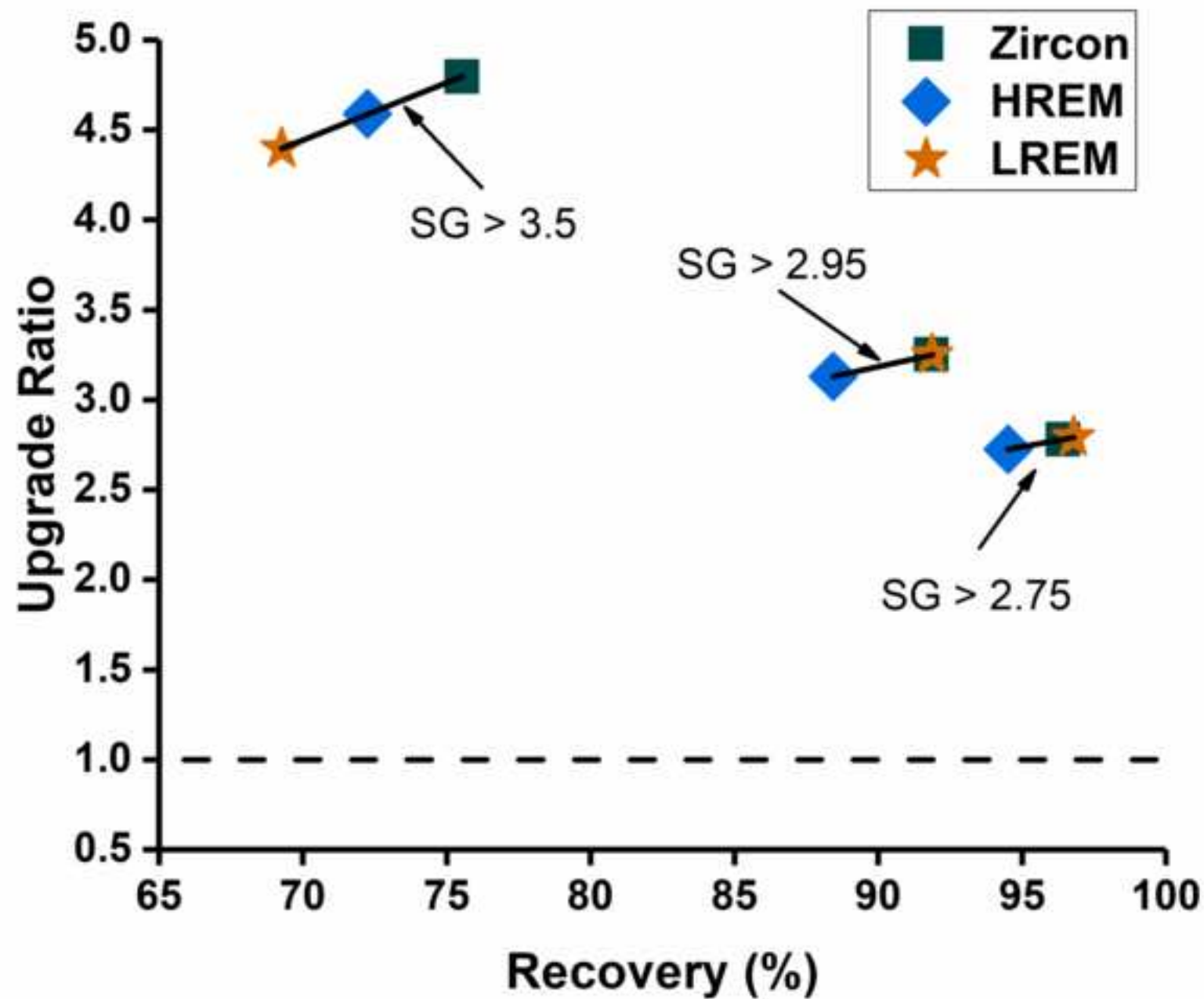




Figure 4  
[Click here to download high resolution image](#)

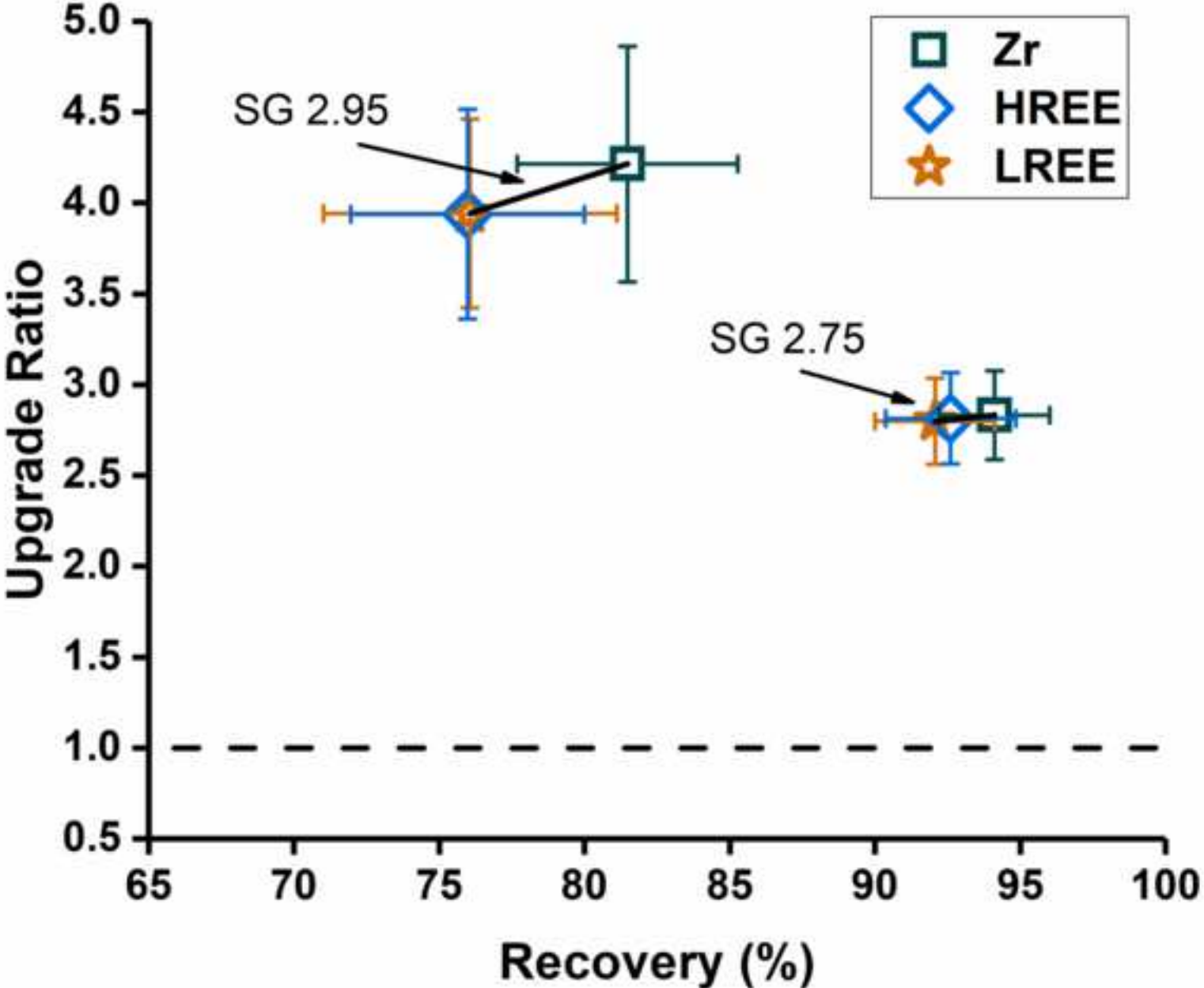
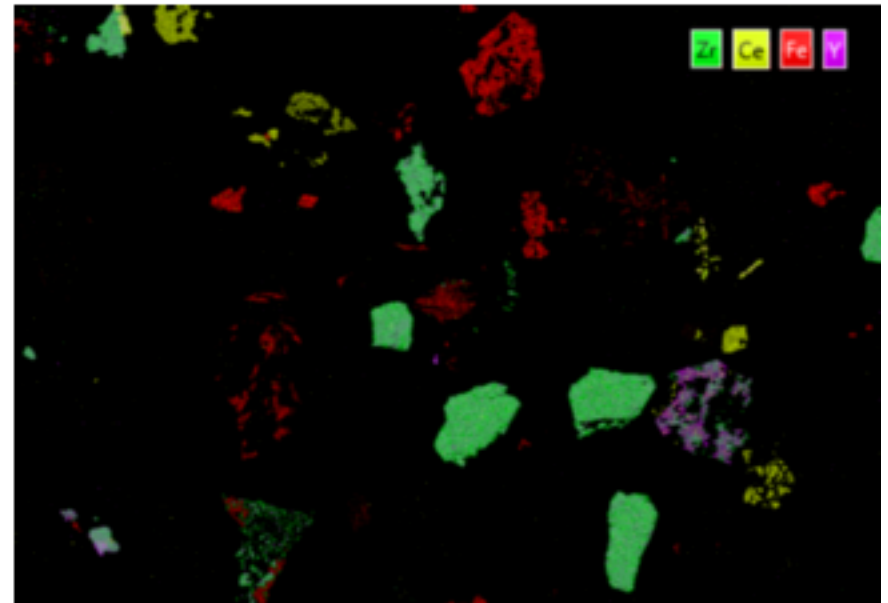
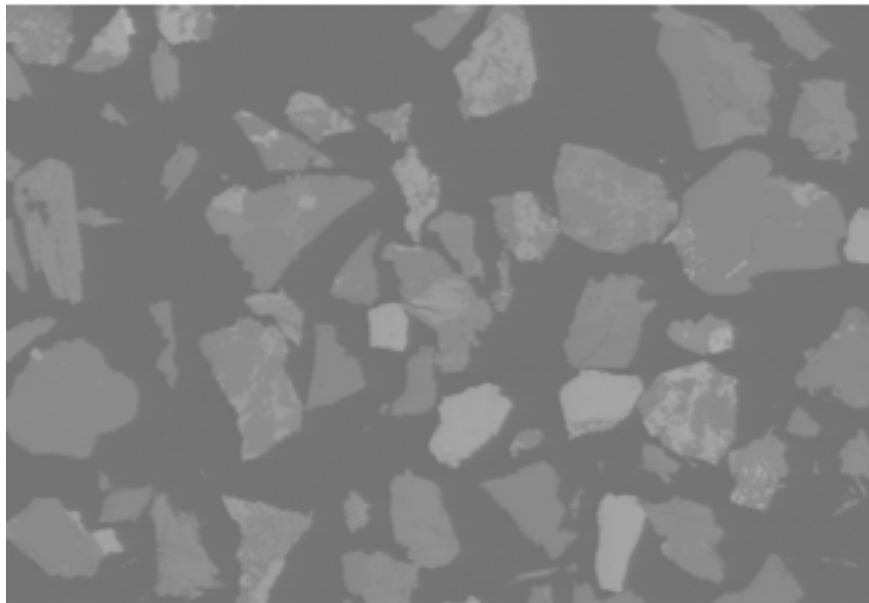




Figure 5  
[Click here to download high resolution image](#)

**Sink**



**Float**

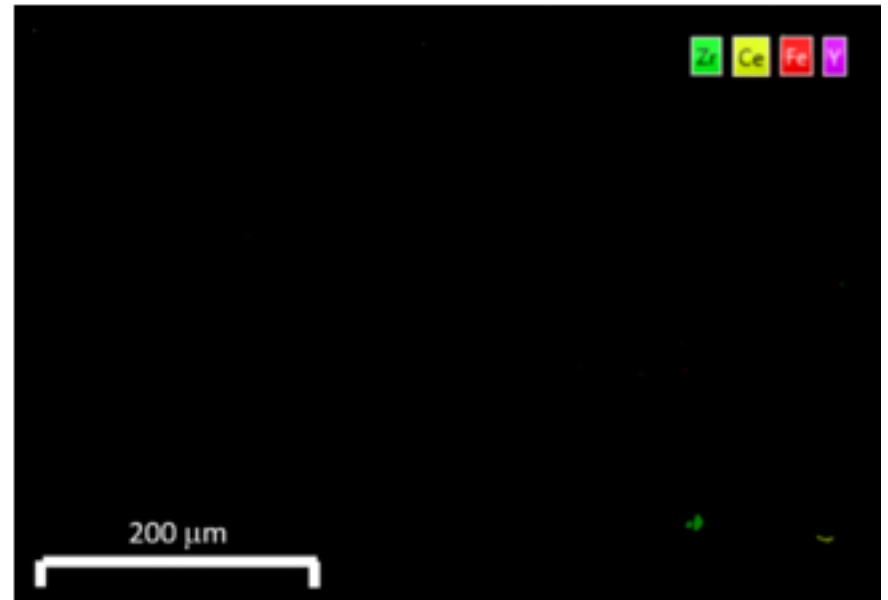


Figure 6  
[Click here to download high resolution image](#)

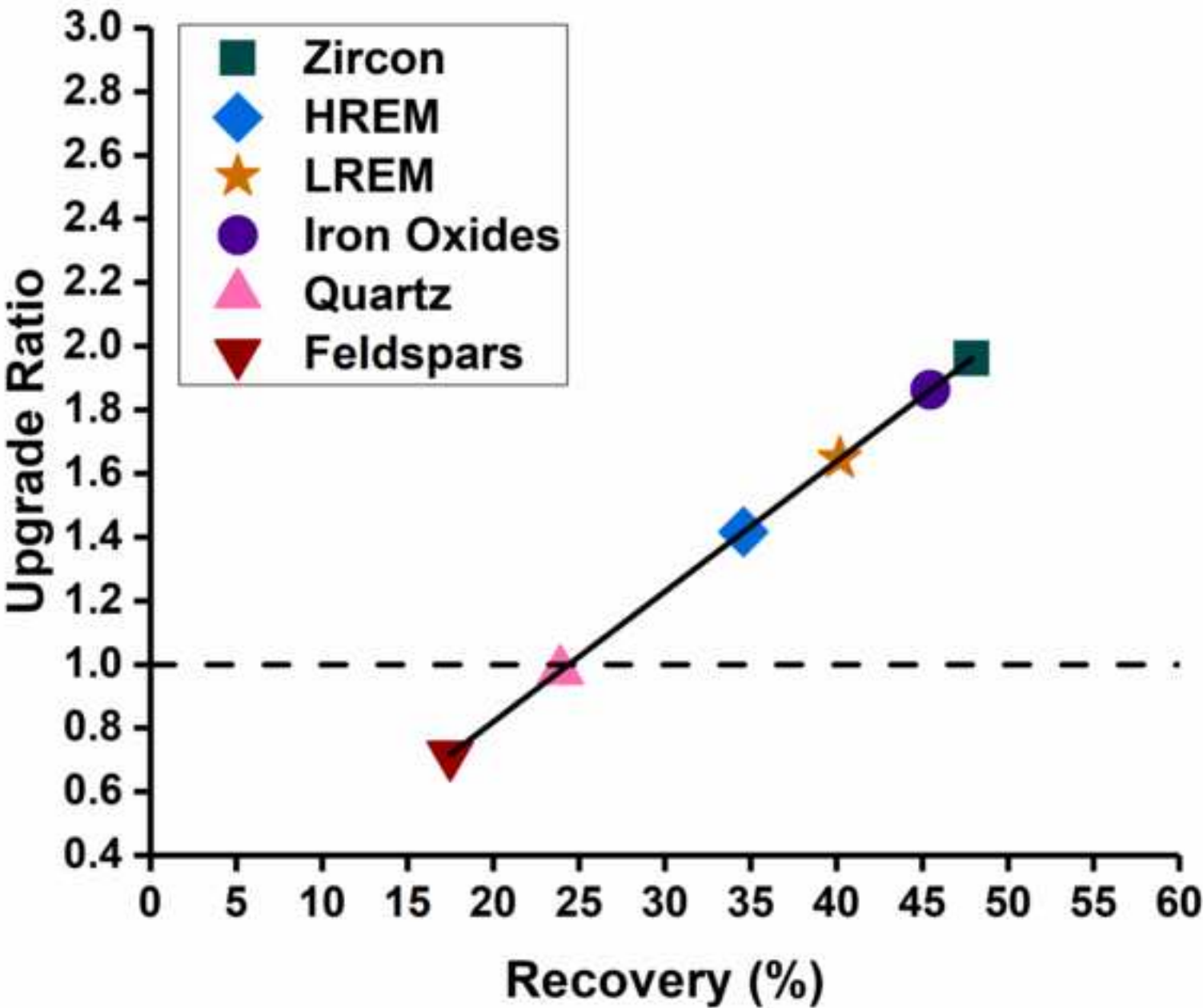
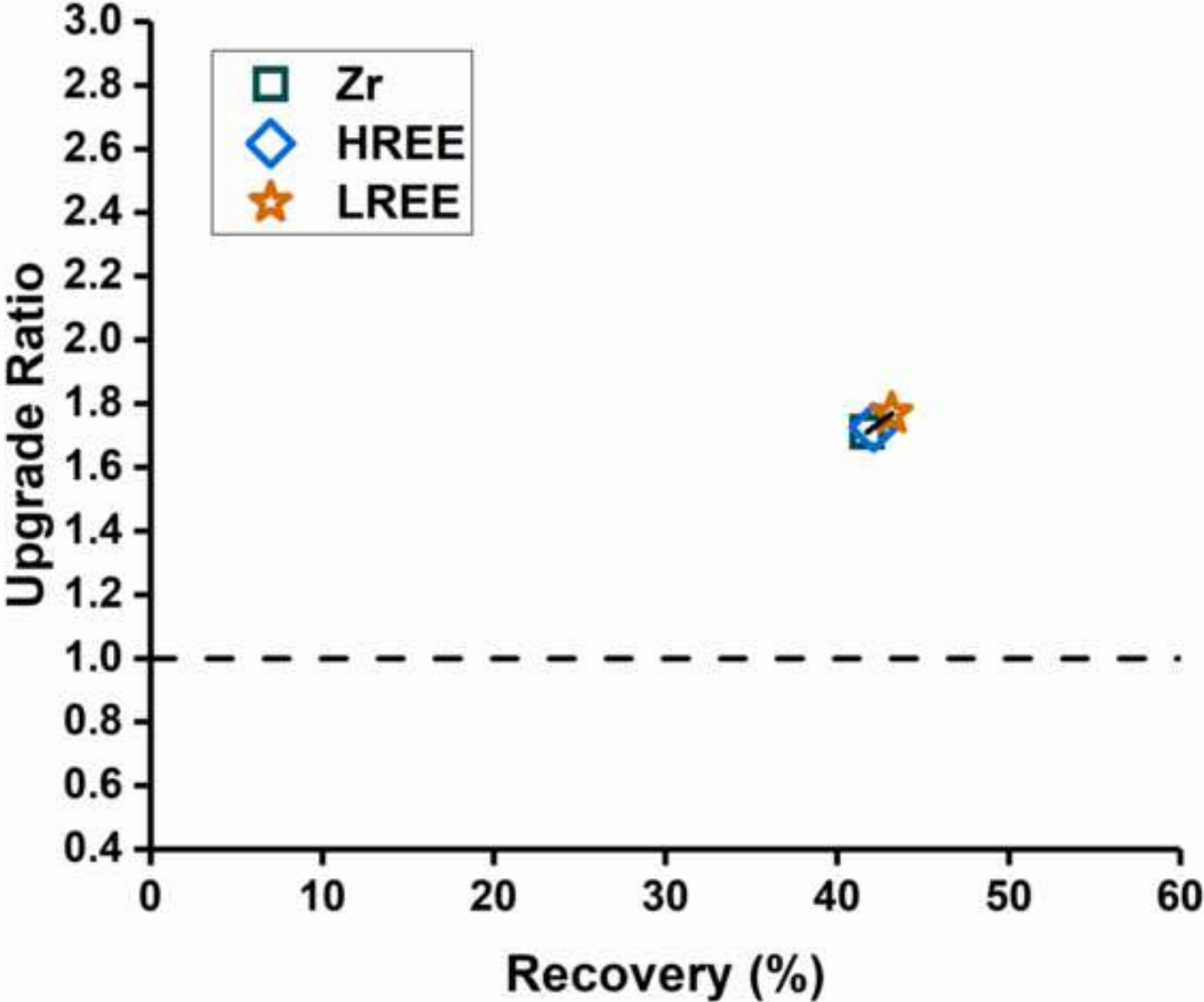


Figure 7  
[Click here to download high resolution image](#)



**Figure 8**  
[Click here to download high resolution image](#)

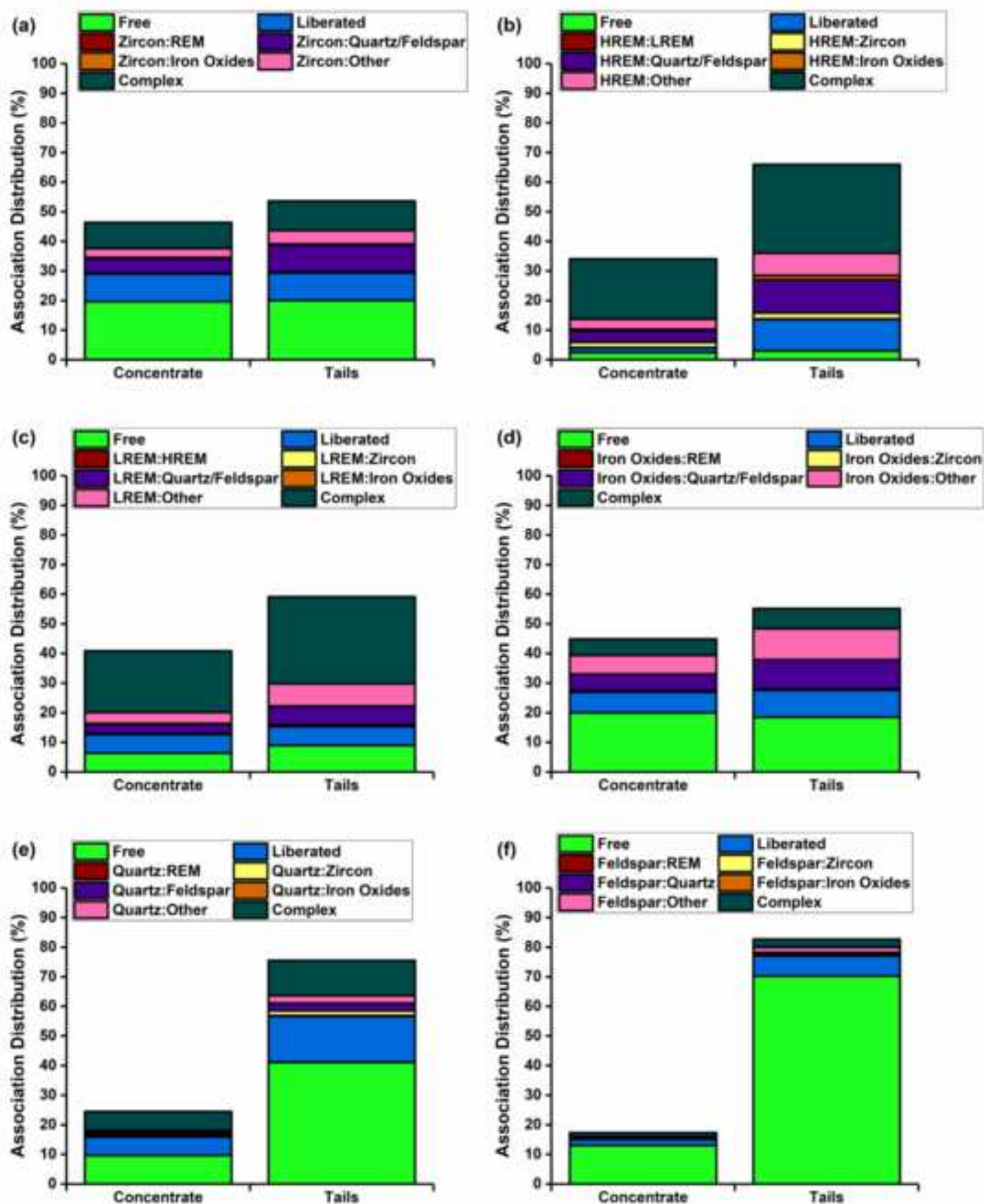


Figure 9  
[Click here to download high resolution image](#)

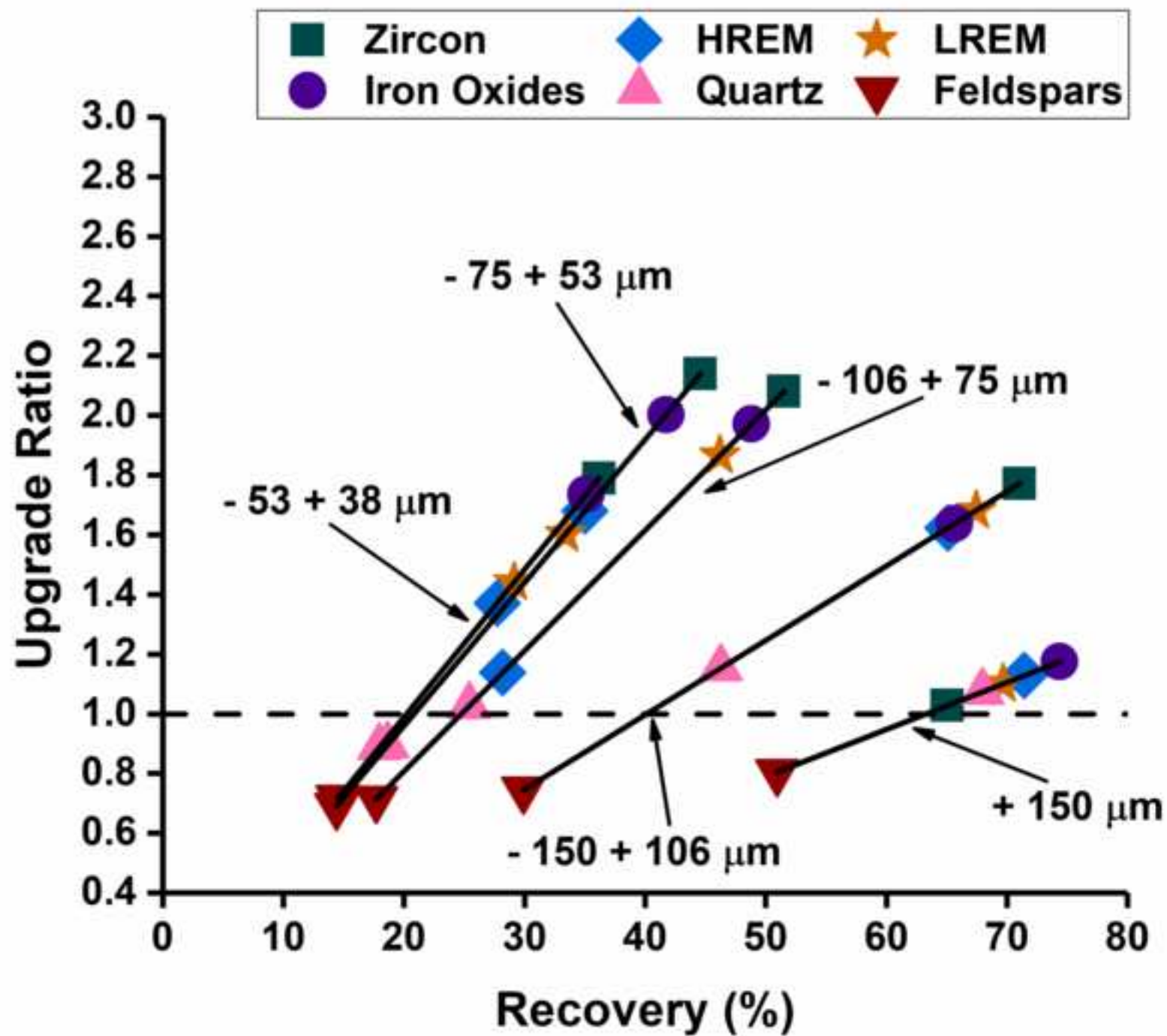


Figure 10  
[Click here to download high resolution image](#)

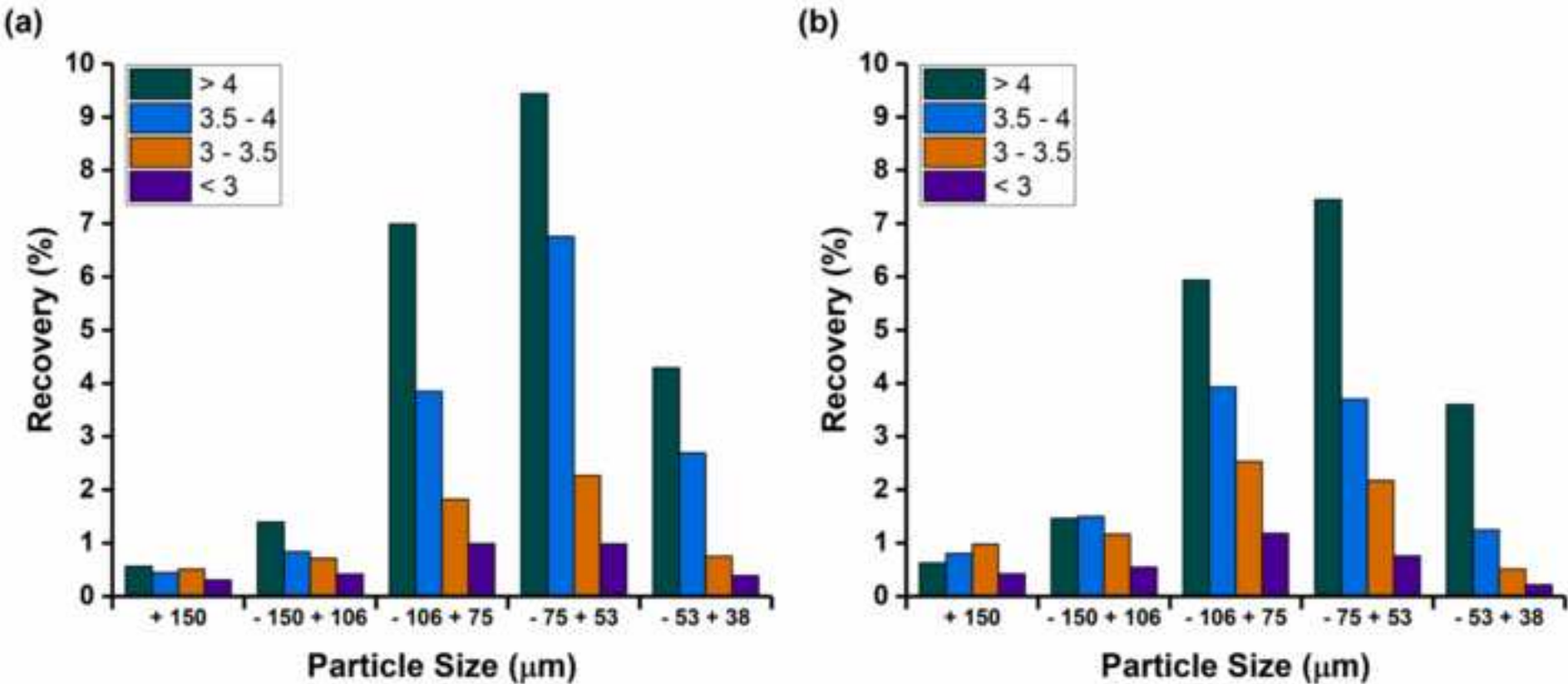




Figure 11  
[Click here to download high resolution image](#)

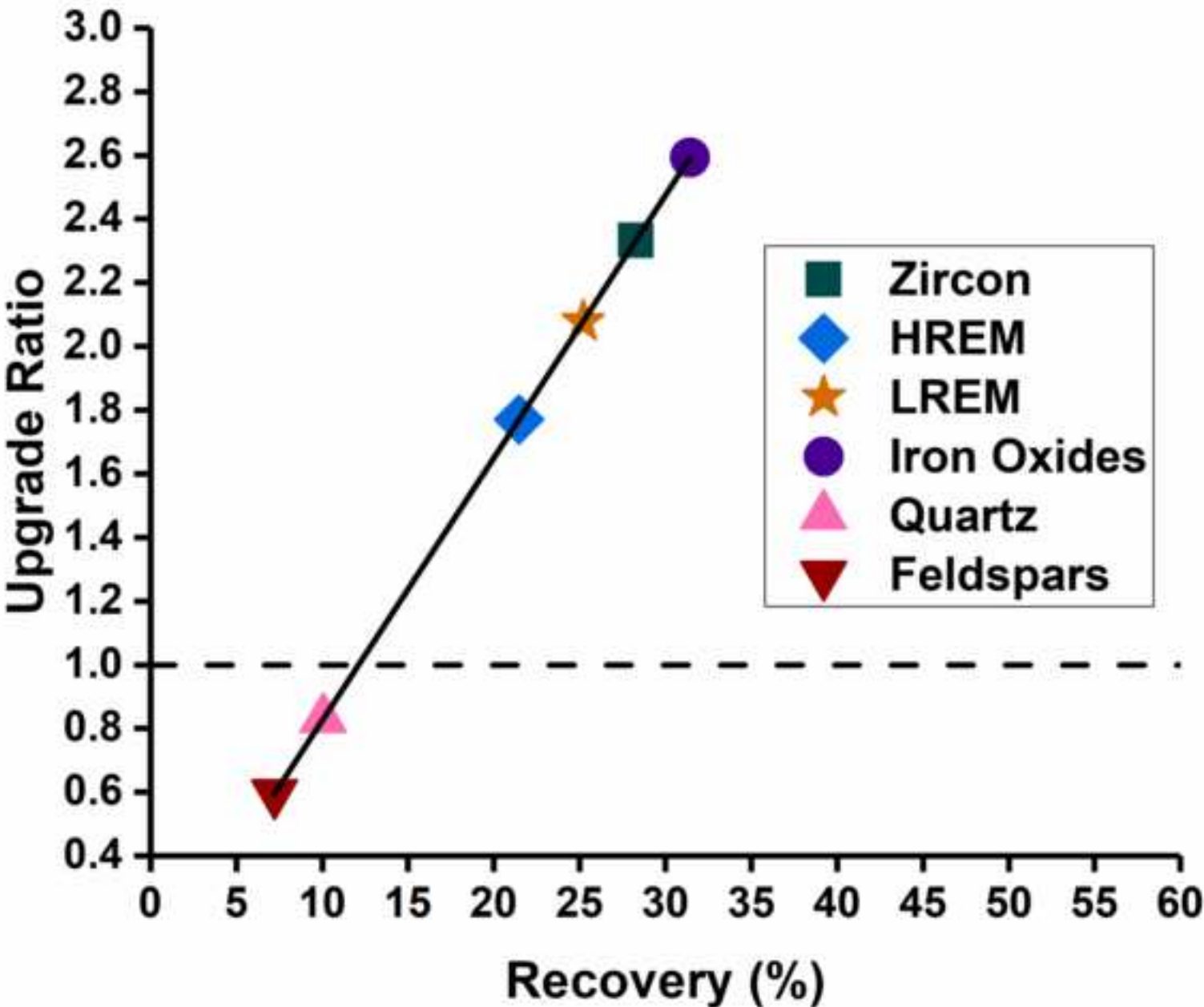


Figure 12  
[Click here to download high resolution image](#)

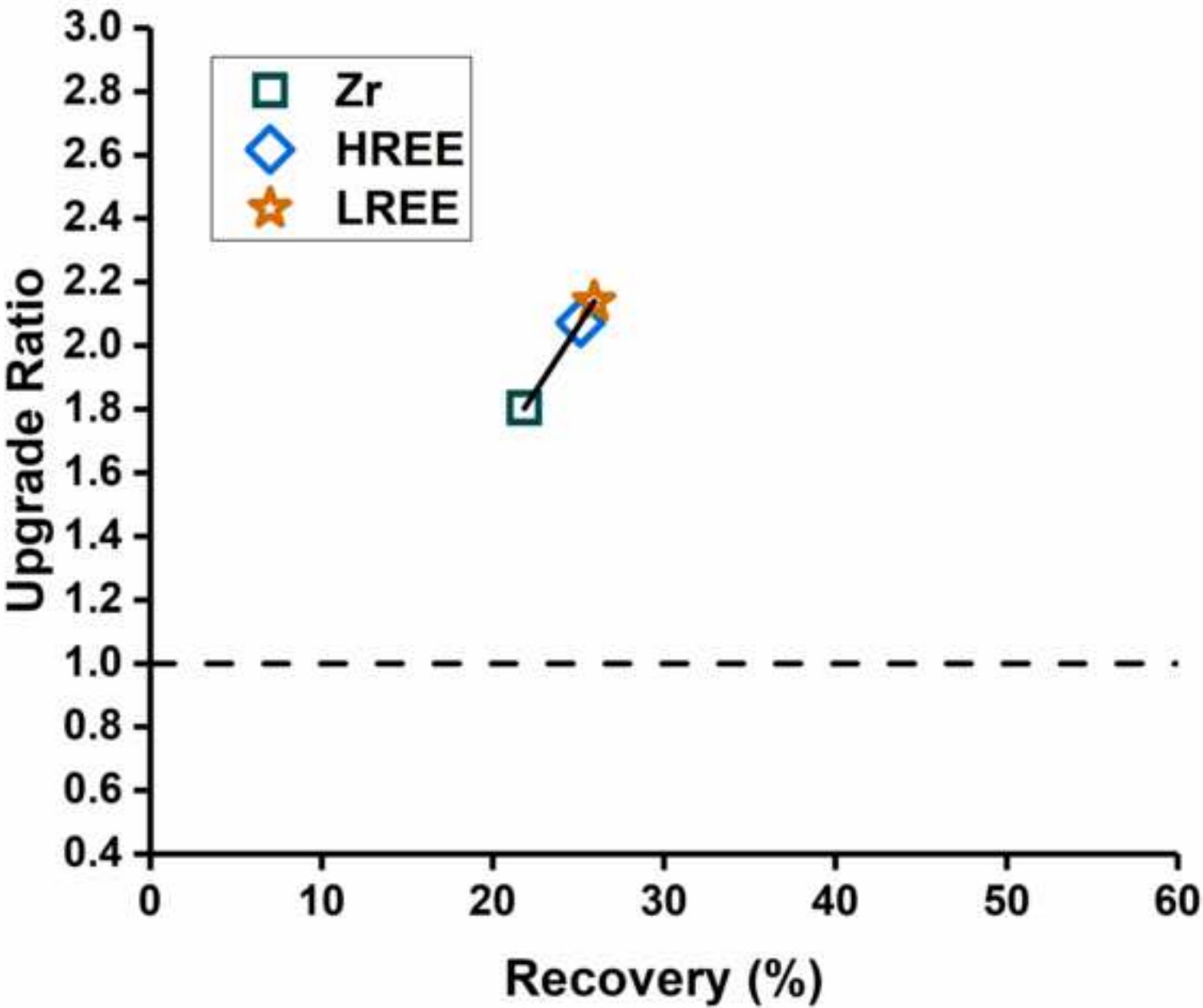




Figure 13  
[Click here to download high resolution image](#)

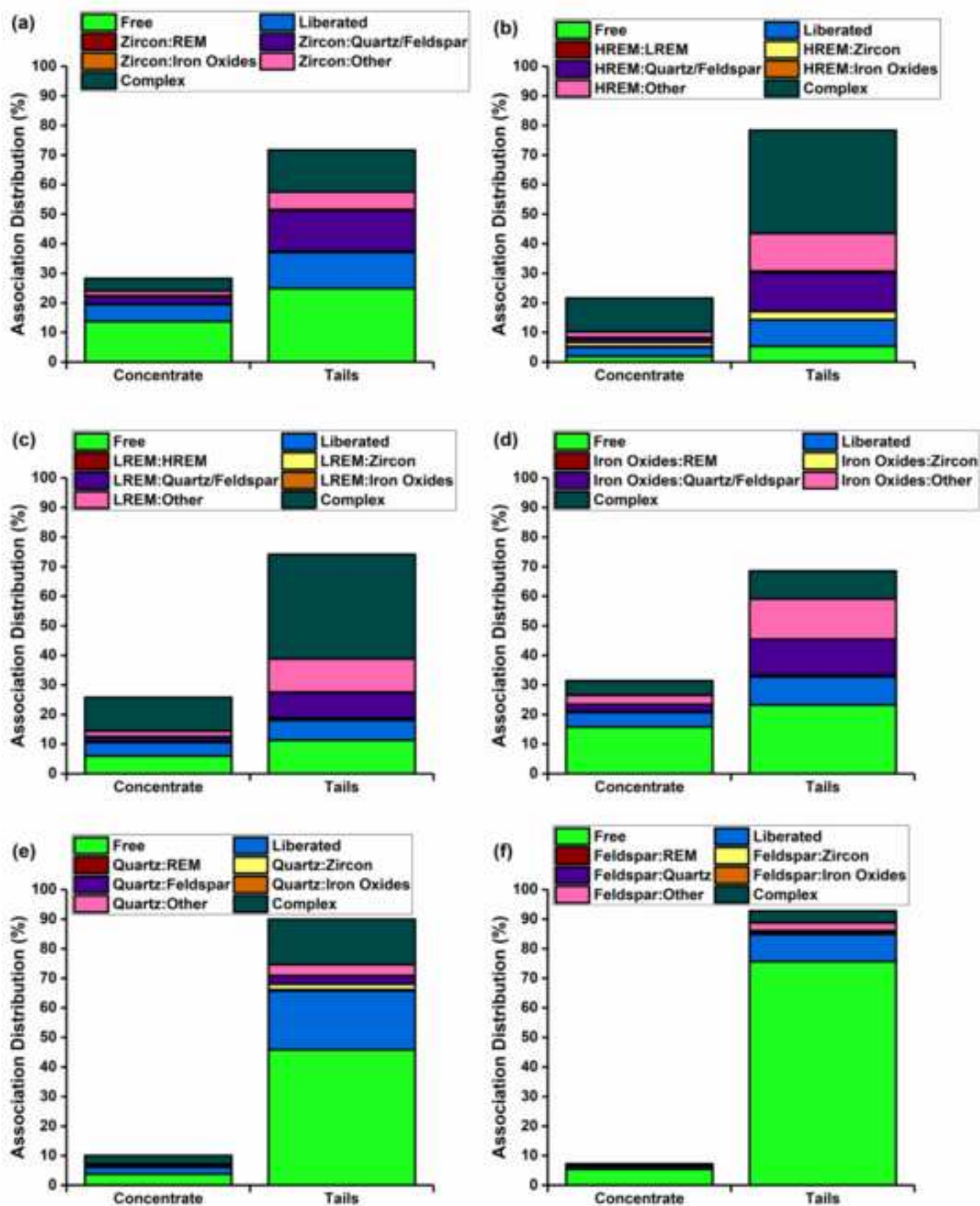


Figure 14

[Click here to download high resolution image](#)

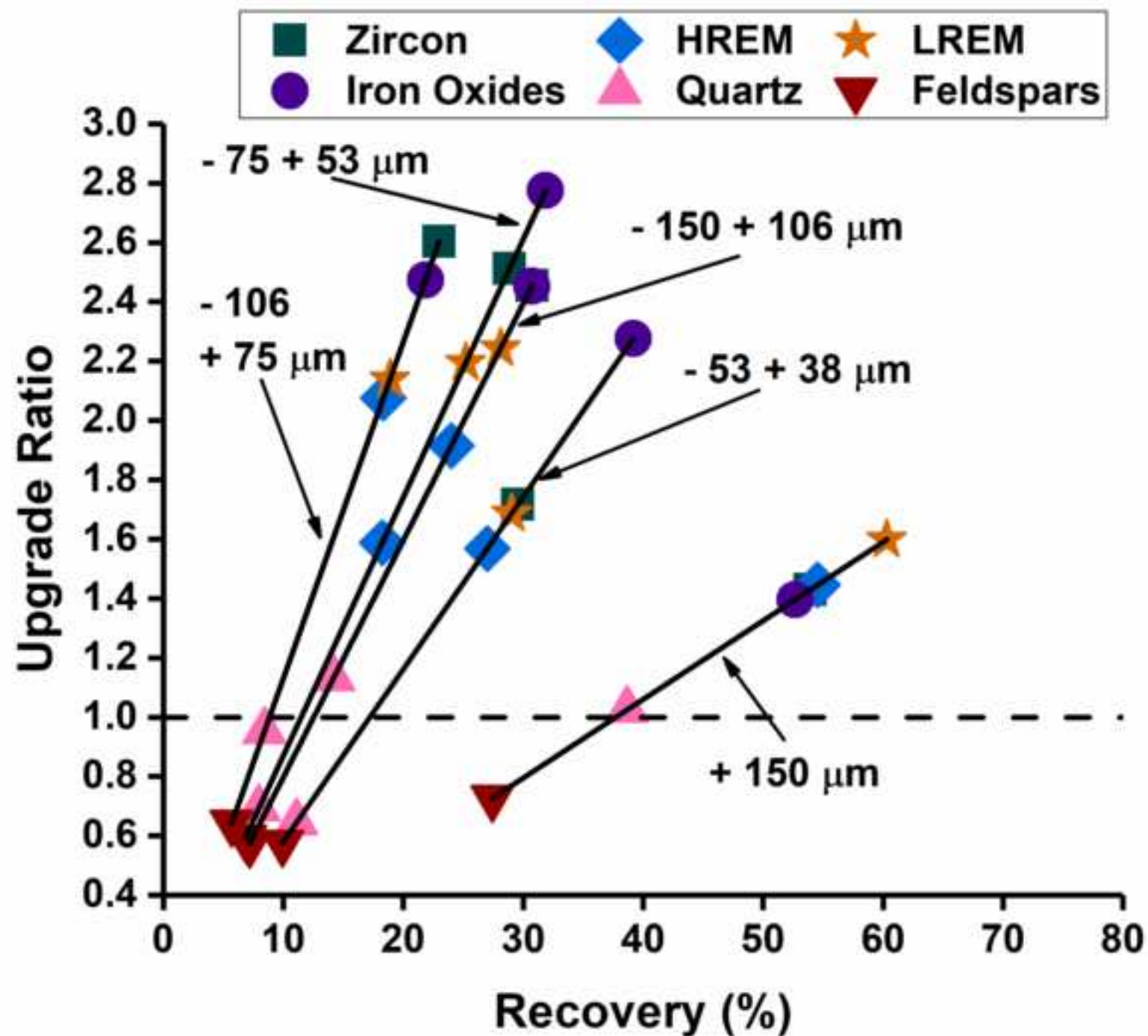


Figure 15  
[Click here to download high resolution image](#)

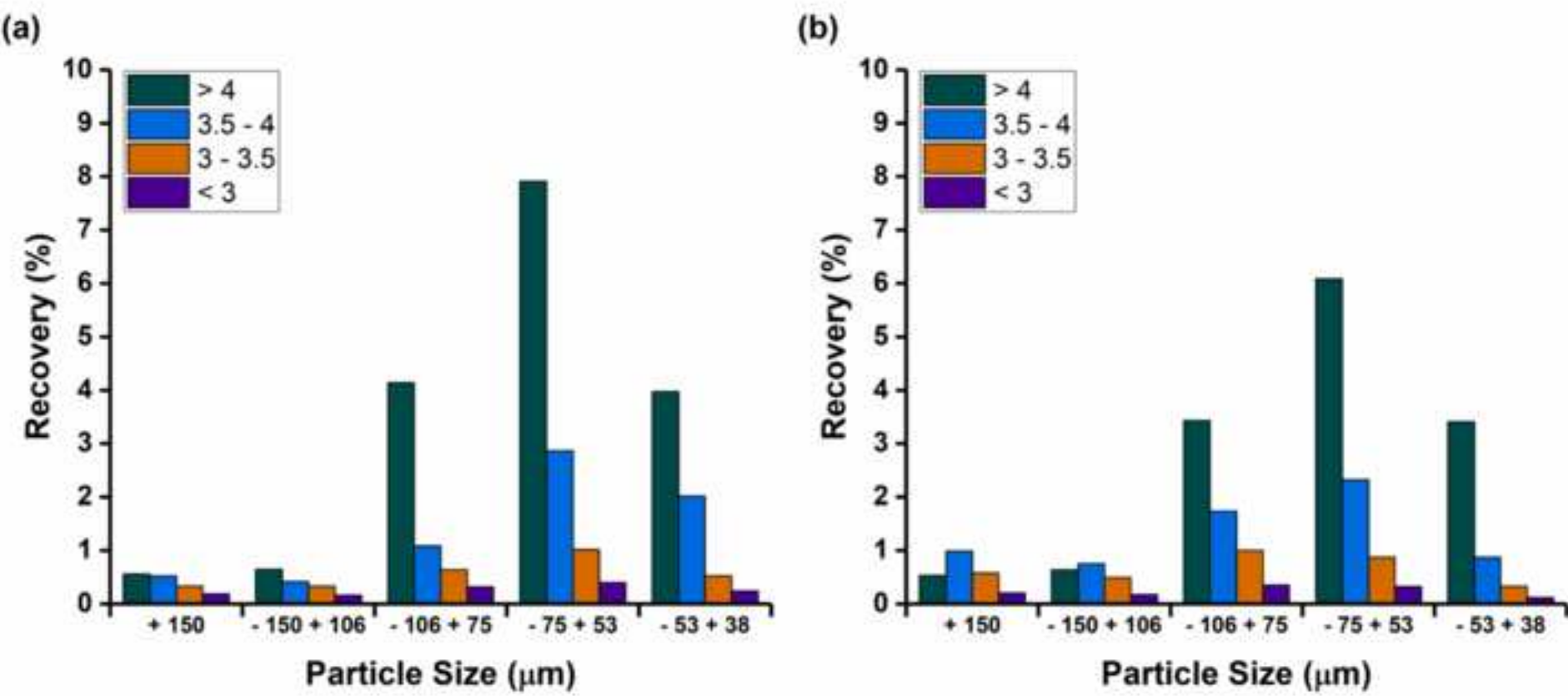


Figure A1  
[Click here to download high resolution image](#)

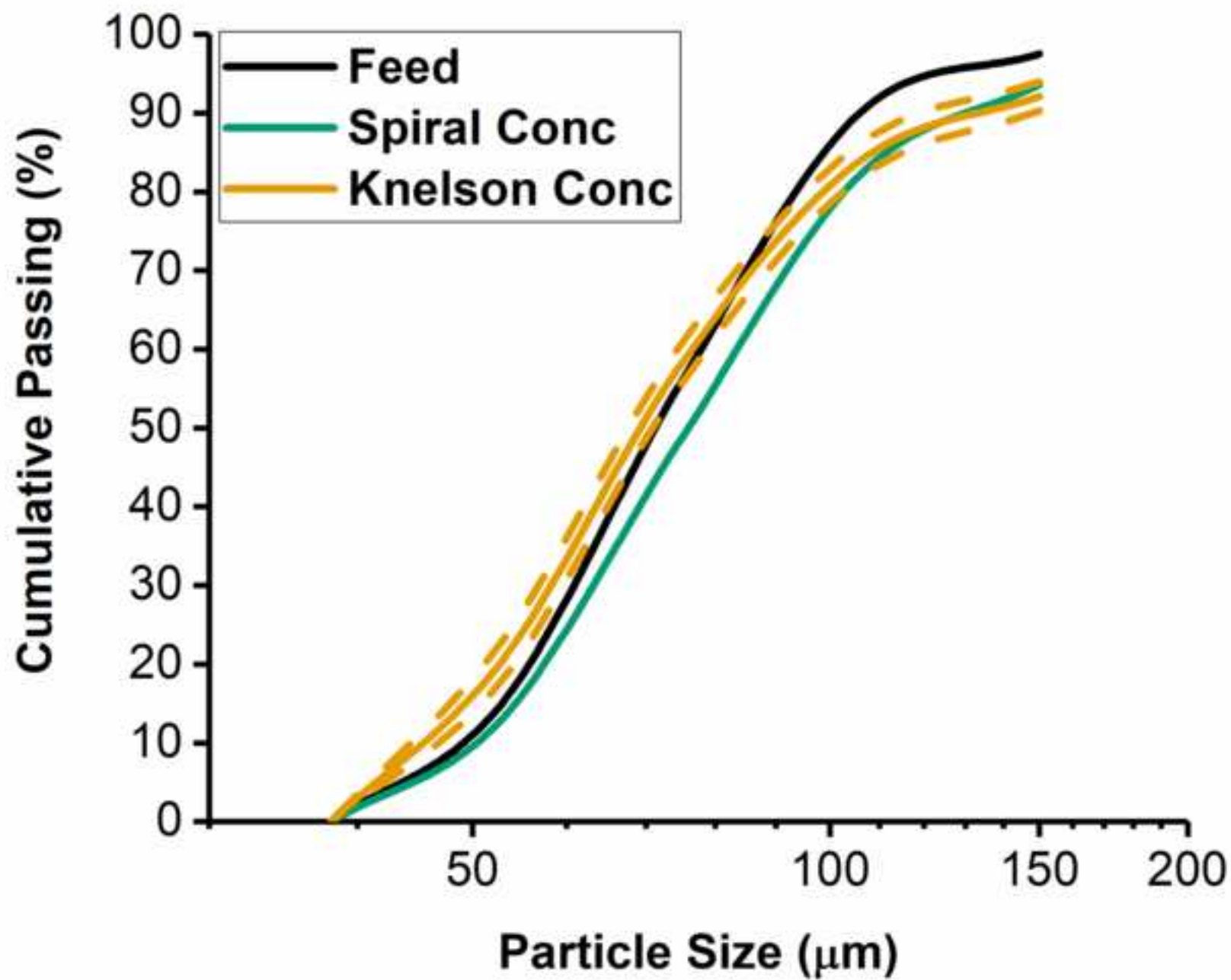




Figure A2  
[Click here to download high resolution image](#)

